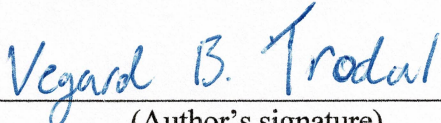




Universitetet
i Stavanger

FACULTY OF SCIENCE AND TECHNOLOGY

Bachelor's thesis

Study program/specialization: Bachelor of Science in Petroleum Engineering	Spring semester, 2021 Open access
Author: Vegard Bror Trodal	 (Author's signature)
Supervisor(s): Dr. Mahmoud Khalifeh Dr. Arild Saasen	
Title of bachelor's thesis: Using ceramic discs to evaluate fluid loss and formation damage	
Credits: 20 ECTS	
Keywords: Fluid loss, permeability, ceramic disc, solids and fibers.	Number of pages: XI + 34 + supplemental material/other: 24 Stavanger, 15th May 2021

Using Ceramic Discs to Evaluate Fluid Loss and Formation Damage

By

Vegard Bror Trodal

Bachelor's Thesis

Presented to the Faculty of Science and Technology

The University of Stavanger

THE UNIVERSITY OF STAVANGER

MAY 2021

Foreword

The research presented in this thesis is part of a larger research project initiated by the European Mud Company (EMC). The work was conducted at EMC's lab located in Forus, Stavanger. Some of the results have been published in a research article, *Klungtveit, K.R., Saasen, A., Vasshus, J.K., Trodal, V.B., Manda, S.K., Berglind, B. and Khalifeh, M., "The Fundamental Principles and Standard Evaluation for Fluid Loss and Possible Extensions of Test Methodology to Assess Consequences for Formation Damage", Energies, 14(8), paper 2252, 2021. <https://doi.org/10.3390/en14082252>*, where I am the 4th author. The article is attached in Appendix C.

Acknowledgement

I would like to thank the great people at European Mud Company for providing an excellent learning experience. Karl Ronny Klungtveit has been essential in this experience, never hesitating to provide insight and helpful advice. Bjørn Berglind was always a pleasure to work alongside in the lab and gave me insight and knowledge from his impressive experience in the field. Jan Kristian Vasshus has his own way of boosting morale and provided practical solutions to improve testing procedures.

I would also like to thank my professors, Arild Saasen and Mahmoud Khalifeh. Your engaging lectures sparked my interest in the field, effectively putting me on this path. I am grateful for all the advice and encouragement you have given me this past year.

Abstract

To prevent kicks and possible blowout of the well, the pressure from the drilling fluid must be kept above the pore pressure of the formation. This differential pressure forces the fluid into the porous formation, which results in fluid loss. Occasionally, the pressure can also exceed the formation fracturing pressure, leading to lost circulation. In both cases, fluid migrates into the formation, potentially causing damage in the process. This study investigated the relationship between filtration volume and formation damage. The methodology is centered around using porous discs to measure fluid filtrate and changes in permeability and mass of the discs. Fifteen samples of drilling fluid were created with different solid, polymer and fiber content. Filtrate volume was recorded by conducting a HTHP fluid loss test with a differential pressure of 6.9 MPa (1000 psi), at 90 °C for 30 minutes. The discs were weighed in dry conditions at the start and end of the test procedure to measure the mass of the invasion caused by the filtrate. Changes in permeability to both water and air was determined, which combined with invasion mass, serve as indicators of formation damage. The results show how the different additives may improve the sealing capabilities and reduce filtrate volume but does not necessarily correlate with reducing invasion and damage to the formation.

Acronyms

AHR – After hot rolling

BHR – Before hot rolling

ECD – Equivalent circulating density

HTHP – High-temperature high pressure

PAC – Polyanionic cellulose

List of Contents

Foreword	iii
Acknowledgement	iv
Abstract	v
Acronyms	vi
List of Contents.....	vii
List of Figures.....	ix
List of Tables.....	xi
1 Introduction	12
1.1 Objective.....	15
2 Methodology.....	16
2.1 Mud preparation.....	17
2.2 Fluid loss procedure	19
2.3 Formation damage.....	20
2.3.1 Filter cake removal	20
2.3.2 Disc mass	21
2.3.3 Permeability	22
3 Results and Discussion.....	23
3.1 Effect of different solids	24
3.1.1 The effect of different solids on viscosity profiles.....	24
3.1.2 The effect of different solids on fluid loss	25
3.1.3 The effect of different solids on disc mass	26
3.1.4 The effect of different solids on permeability.....	27
3.2 Effect of adding fibers.....	28
3.2.1 The effect of adding fibers on viscosity profiles.....	28
3.2.2 The effect of adding fibers on fluid Loss.....	30
3.2.3 The effect of adding fibers on disc mass	31

3.2.4 The effect of adding fibers on permeability	32
3.3 Effect of different polymers.....	33
3.3.1 The effect of using different polymers on viscosity profiles	33
3.3.2 The effect of using different polymers on fluid loss	36
3.3.3 The effect of using different polymers on disc mass.....	37
3.3.4 The effect of using different polymers on permeability	38
3.4 Different concentration of CaCO ₃ and different median pore sizes	39
3.4.1 The effect of increasing concentration of CaCO ₃ on viscosity profiles	39
3.4.2 The effect of increasing concentration of CaCO ₃ and median pore size on fluid loss.....	41
3.4.3 The effect of increasing concentration of CaCO ₃ and median pore size on disc mass	42
3.4.4 The effect of increasing concentration of CaCO ₃ and median pore size on permeability.....	43
4 Conclusion.....	44
5 References	45
Appendix A - Recipes	46
Appendix B – Example of permeability calculations	48
Appendix C – Research article	50

List of Figures

Figure 1 - OFITE ceramic discs. 20 μ m disc to the left and 50 μ m disc to the right.....	16
Figure 2 - To the left is the scale, Ohaus ax1502, used for measuring all components. To the right is the Hamilton beach mixer.	18
Figure 3 - OFITE Viscometer model 900.	18
Figure 4 - To the left is the OFITE HTHP Filter Press in parts. Used for conducting fluid loss tests. To the right is the scale and a measuring cylinder used for recording the fluid loss.	19
Figure 5 - Custom setup for filter cake removal and permeability measurements.....	20
Figure 6 - OHAUS MB120 moisture analyzer. Used for removing moisture and determining disc mass.	21
Figure 7 - Ceramic disc mounted in acrylic cylinder.....	22
Figure 8 - Shear stress versus shear rate for solid free, bentonite, calcium carbonate and micronized barite samples.....	24
Figure 9 - Fluid loss results for solid free, bentonite micronized barite and calcium carbonate (Samples 1-4).	25
Figure 10 - Increase in mass of the ceramic discs used with solid free, bentonite, calcium carbonate and micronized barite.	26
Figure 11 - Retained permeability to water and air for solid free, bentonite, micronized barite and calcium carbonate (Sample 1 to 4).....	27
Figure 12 - Shear stress versus shear rate for solid free fluid, with and without fiber (Sample 1 and 5).....	28
Figure 13 - Shear stress versus shear rate for bentonite fluid, with and without fiber (Sample 2 and 6).....	28
Figure 14 - Shear stress versus shear rate for calcium carbonate fluid, with and without fiber (Sample 3 and 7).	29
Figure 15 - Shear stress versus shear rate for micronized barite fluid, with and without fiber (Sample 4 and 8).	29
Figure 16 - Spurt fluid loss for solid free, bentonite, micronized barite and calcium carbonate, with and without fiber (Sample 1-8).....	30
Figure 17 - Total fluid loss for solid free, bentonite, micronized barite and calcium carbonate, with and without fiber (Sample 1-8).....	30

Figure 18 - Increase in disc mass for solid free, bentonite, micronized barite and calcium carbonate, with and without fiber, (Sample 1-8).....	31
Figure 19 - Retained permeability to water for solid free, bentonite, micronized barite and calcium carbonate, with and without fiber (Sample 1 to 8).	32
Figure 20 - Retained permeability to air for solid free, bentonite, micronized barite and calcium carbonate, with and without fiber (Sample 1 to 8).....	32
Figure 21 - Shear stress versus shear rate for Polymer A and PAC combination (Sample 9).....	33
Figure 22 - Shear stress versus shear rate for Polymer A and Polymer B combination (Sample 10).....	34
Figure 23 - Shear stress versus shear rate for Polymer A and Starch combination (Sample 11).....	34
Figure 24 - Shear stress versus shear rate for Xanthan gum and PAC combination (Sample 12 and 13).....	35
Figure 25 - All fluid loss results for the different polymer combinations (Sample 9 to 13).....	36
Figure 26 - Disc mass increase using different polymer combinations (Samples 9-13).	37
Figure 27 - Retained permeability to air and water using different polymer combinations (Samples 9-13).	38
Figure 28 - Shear stress versus shear rate for fluids with different concentrations of calcium carbonate (Sample 3 and 14).....	39
Figure 29 - Shear stress versus shear rate for fluids with fiber and different concentrations of calcium carbonate (Sample 3 and 14).....	40
Figure 30 - Fluid loss results different concentration of calcium carbonate, and different median pore sizes. (Samples 3, 7, 12-15)	41
Figure 31 - Increases in disc mass for different concentration of calcium carbonate, and different median pore sizes. (Samples 3, 7, 12-15).....	42
Figure 32 - Retained permeability to water and air for different concentration of calcium carbonate, and different median pore sizes. (Samples 3, 7, 12-15).....	43

List of Tables

Table 1 - Components used in drilling fluid samples.	17
Table 2 - Overview of tests and samples.....	23

1 Introduction

During well construction, drilling fluid acts as the primary barrier of the wellbore and is a key component in most drilling operations. The fluid is pumped downhole through the drill string and ejected through nozzles at the drill bit. In this process one of the main functions of the drilling fluid is fulfilled, to cool and lubricate the bit. The nozzles are relatively small compared to the drill string, which causes the velocity of the fluid to be much higher at the outlet. This leads to a jet impact force which helps crack the formation at the bottomhole and facilitates the rate of penetration. As the drill bit penetrates the formation, rock fragments of varying sizes are created, called cuttings. These need to be removed from the hole, and drilling fluid serves a crucial role also in this process. The cuttings are suspended in the fluid and transported to the surface through the annular space between the drill string and the formation. To achieve these functionalities the rheological properties of the fluid are important. For drilling, a shear-thinning fluid is often desirable, meaning that the viscosity is decreasing with increasing shear stress. This enables easy flow through the nozzles where the shear stress is high, while also making the fluid more viscos in the more spacious annulus, which enables transportation of the cuttings. It must also have a gel strength to minimize sag of cuttings and solid additives in the event of a circulation stop.

Another crucial functionality of drilling fluid is maintaining wellbore stability and preventing incidents such as kicks, blowout and collapse of the borehole. When creating a hole, the pressure of the surrounding formation will try to fill it. It is therefore necessary that the mud column provides a hydrostatic pressure that equalizes the pressure from the formation. This is achieved by continuously adjusting the density of the drilling fluid such that the equivalent circulating density is kept between the pore pressure and the fracture pressure [1]. Equivalent circulating density (ECD) is the effective density of the fluid and combines the measured density and the pressure drop in the annulus. By keeping the ECD above the pore pressure, fluid will naturally escape into the porous formation, resulting in filtration loss. As drilling fluid is pushed into the formation, particles larger than the pore openings will be deposited on the wall and form a filter cake. It is desirable that the filter cake is as impermeable and thin as possible to prevent further fluid loss and a stuck pipe situation.

There are many factors involved when estimating the fracturing pressure and pore pressure of the formation, making it difficult to calculate precisely. As a result of this uncertainty the ECD will sometimes exceed the fracturing pressure which can cause existing fractures to grow or new fractures to be created. This can lead to severe fluid loss and lost circulation, as less mud returns to the mud pits than what is pumped downhole. Similarly, in high permeable zones the pore pressure may be much lower than the hydrostatic pressure from the mud column, resulting in the loss of drilling fluid. Lost circulation is not only costly but can lead to many drilling-related problems. It is therefore necessary to prevent or minimize the risk of this occurring. One way this is done is by regularly conducting formation integrity tests and leak-off tests to verify the strength of the formation. Adding bridging agents or lost circulation material to the drilling fluid is another solution to the problem. These additives can prevent or remedy fluid loss by sealing pore throats and fractures. In 2014, Alsaba et al. [2] studied the performance of conventional LCM in creating an effective seal and reduce fluid loss. They found that fibrous materials showed the best performance and considered the reason to be the irregular shape of the fibers and the broad particle size distribution.

An issue with fluid loss is that it can cause damage to the formation. Fines and additives used in the drilling fluid, such as solid particles and polymers, can migrate with the filtrate into the formation [3]. This invasion can plug the pores resulting in reduced permeability. This is especially undesirable in near reservoir formations, as reduced permeability results in lower productivity and affects the economic viability. It is therefore necessary to engineer the drilling fluid, such that fluid loss is minimized.

When creating a drilling fluid there are many factors to consider. It must have the right rheological properties to ensure good flow and transportation of cuttings, while also keeping the borehole stable and safe. To achieve these desired properties, a range of additives are used. Polymers are often added for rheological properties and to reduce fluid loss. Among these, xanthan gum, starch and polyanionic cellulose (PAC) are commonly used in water-based drilling fluids. Khan et al. [4] showed that these polymers might reduce fluid loss to the formation. However, they have little effect in preventing solids from entering the formation when the pore-throat size is larger than $20\mu\text{m}$, and differential pressure exceeding 3.45 MPa (500 psi). Different solids are also added to give the fluid various properties. Barite is a very dense material and is added to increase the density and thereby the hydrostatic pressure of the mud column. Calcium carbonate can also be used as a weighting material but is more commonly

used as a bridging agent to increase the sealing capabilities of the filter cake and thus reduce fluid invasion in permeable zones.

While there are a range of different additives available, creating a perfect drilling fluid is an impossible task. This is partly because every well is different, and the conditions downhole may change from what is expected at any point. It is therefore important for the mud engineer to continuously monitor, test and adjust the drilling fluid. Testing is done on-site during the operation, and also in lab conditions for research purposes. ANSI/API 13B-1 [5] describes industry standards for testing water-based drilling fluids. Fluid loss tests are typically conducted as either API filter press or HTHP fluid loss test. Normal test conditions for HTHP are 66 °C (150 F) and 3.45 MPa (500 psi).

Core flooding is a conventional method for testing formation damage caused by drilling fluids. In 2017, Green et al. [6] studied core flooding at reservoir conditions using oil-based mud in order to design drilling and completion fluids for a Norwegian field. They concluded that permeability alterations caused by the drilling fluid were limited to the first few pores from the wellbore, regardless of total fluid loss volume and thickness of the filter cake. Additionally, they found no direct connection between the amount of fluid loss volume and formation damage. A study conducted by Nelson in 2009 [7] investigated the pore sizes in siliciclastic rocks. He found that the typical pore sizes in reservoir sandstones were greater than 20µm and the pore throat size greater than 2µm. Both the data from Nelson and Green et al. underpins the possibility of using ceramic discs with median pore throat size of 20µm in evaluating permeability changes near the wellbore in reservoir formations.

Klungtvedt et al. [8] presented the performance of two Non-Invasive Fluid (NIF) additives in a KCl polymer drilling fluid. The testing included HTHP fluid loss tests at 90°C (194 F) and 3.45 MPa (500 psi) using ceramic discs with median pore sizes of 20µm and 50µm. They were successful in using an oxidizing breaker solution to remove the filter cake. Additionally, they found that weighing the ceramic discs at different stages during testing could provide useful information regarding the invasion and possible formation damage. A similar approach was used for the research presented in this thesis. The experimental method was also set up around a typical HTHP test and measuring changes in disc mass. However, it was expanded to include changes in permeability, in order to get a better understanding of the relationship between fluid loss and formation damage. Some of the results are presented in

Klungtvedt et al. [9]. This study will use the same method to investigate further the connection between filtration volume and damage to the formation.

1.1 Objective

Lost circulation can lead to many drilling-related problems, and cause damage to the formation. The conventional methods for evaluating fluid loss do not provide any information regarding formation damage. While core flooding can be used to measure changes in permeability, it is both time-consuming and expensive. This study aims to use the method by Klungtvedt et al. [9] to evaluate:

- What effect different solids, polymers and fiber used in drilling fluids, have on fluid loss, particle invasion and permeability.
- Whether there is a relationship between filtrate volume from the HTHP test, invasion of particles and changes in permeability, in near wellbore formations.

2 Methodology

The methodology for evaluating fluid loss and formation damage is formed and adjusted over the course of over 100 tests, and the results from 15 of them will be presented. These tests are centered around ceramic discs with median pore sizes of $20\mu\text{m}$ and $50\mu\text{m}$, and include fluid loss tests, permeability measurements and changes in disc mass. Examples of ceramic discs used are shown in **Figure 1**.



Figure 1 - OFITE ceramic discs. $20\mu\text{m}$ disc to the left and $50\mu\text{m}$ disc to the right.

2.1 Mud preparation

For testing the effect of different additives, fifteen samples of water-based drilling fluids were prepared. Table 1 shows all the components used in creating the samples, and a small functionality description. Detailed recipes, including mixing order and duration, are found in Appendix A. The calcium carbonate was sieved, and only particles smaller than 53 μ m was used.

Table 1 - Components used in drilling fluid samples.

Mud component	Functionality
Water	
Soda Ash (Na ₂ CO ₃)	Increase alkalinity.
Caustic Soda (NaOH)	Increase alkalinity.
Magnesium Oxide (MgO)	Prevent drastic reduction in pH during hot-rolling.
Potassium chloride (KCl)	Inhibitor to prevent swelling of bentonite.
Calcium carbonate (CaCO ₃)	Briding agent/lost circulation material.
AURACOAT UF	Fiber based non-invasive lost circulation material.
Micronized barite	Weighing material.
Bentonite	Naturally exists in the formation. Infiltrates the fluid. Acts as a solid.
Starch	Increase viscosity.
Xanthan Gum	Increase viscosity, adds load-bearing capacity.
Polymer A	Modified starch. Increase viscosity at low shear rates. Reduce fluid loss.
Polymer B	Modified starch and cellulose. Reduce fluid loss.
PAC-LV	Reduce fluid loss.

All the components were weighed using Ohaus ax1502, and the mixing was conducted using a Hamilton Beach Mixer, both shown in **Figure 2**. After mixing each sample the pH and rheology were determined. All rheological profiles were determined at 50 °C using OFITE Model 900 viscometer, shown in **Figure 3**. The samples were then put into a hot rolling oven for 16 hours at 90 °C. This simulates the degradation of the drilling fluid flowing through the circulating system. After hot rolling, the samples were spun in Hamilton Beach Mixer for 5 minutes to counteract potential sag during hot rolling, before a final measurement of pH and rheology. This ensures that the properties of the fluid remain intact.



Figure 2 - To the left is the scale, Ohaus ax1502, used for measuring all components. To the right is the Hamilton beach mixer.



Figure 3 - OFITE Viscometer model 900.

2.2 Fluid loss procedure

The fluid loss test was conducted using a high-temperature high-pressure filter press, as shown in **Figure 4**. Before each fluid loss test the ceramic disc was soaked in room temperature water containing 20g/l NaCl. This simulates a porous formation containing brine. After soaking for 30 minutes the disc was inserted into the HTHP cell. 150ml of the sample was added to the cell where it was heated until it reached 90 °C. Then a differential pressure of 6.9 MPa (1000 psi) was applied using a nitrogen gas source. The filtrate was accumulated in a measuring cylinder placed on a scale below the exit valve and recorded at different time intervals for 30 minutes. This setup made it possible to measure both the mass and volume of the filtrate continuously. The results will present the total filtrate volume and the spurt loss, which is defined as the filtrate volume after 30 seconds.



Figure 4 - To the left is the OFITE HTHP Filter Press in parts, used for conducting fluid loss tests. To the right are the scale and a measuring cylinder used for recording the fluid loss.

2.3 Formation damage

Two methods were used to determine potential formation damage caused by different additives in drilling fluid. The first being an increase in mass, which translates into the content of solid particles, polymers and fibers from the drilling fluid remaining in the porous medium. These remains can clog the pores which results in reduced permeability. In order to analyze this, the filter cake had to be removed from the ceramic disc. This was done in two parts, first mechanically by reverse flow of water through the disc, then chemically using a breaker solution.

2.3.1 Filter cake removal

To remove the filter cake and conduct permeability measurements, an experimental setup was developed to allow for the flow of water and air through the disc in the opposite direction than the fluid loss test. The following equipment was used in creating this setup:

- Custom-built transparent acrylic cylinder with mounting
- Festo Pressure regulator LRP-1/4-2.5 and LRP-1/4-0.25
- Festo Pressure Sensor SPAN-P025R and SPAN-P10R
- Festo Flowmeter SFAH-10U



Figure 5 - Custom setup for filter cake removal and permeability measurements.

Figure 5 shows how the setup is assembled. A gas source supplying 0.8 MPa air pressure is connected to the system, and both gas flow rate and pressure can be regulated. The gas enters the cylinder through the top of the lid. An alternative explanation of the setup is found in Appendix C.

For filter cake removal, the ceramic disc is placed into the acrylic cylinder with the filter cake facing down. 1 liter of 60 °C water containing 20 g/l NaCl is added to the cylinder, before a differential pressure of 50 kPa is applied to push the water through the disc. This was repeated once, but with 1 liter of 60 °C fresh water without the addition of NaCl. Removing the filter cake by this method had variable results depending on the drilling fluid used. For some of the tests there were just small remains left on the peripheral of the disc, while in others the filter cake was almost completely intact. As a result of this another method for removing the filter cake was applied to all discs. After the reverse flow, the discs were placed in AURABREAK for 4 hours while holding a temperature of 90-100 °C. This is an oxidizing breaker solution designed to dissolve polymers and fibers and should have little effect on the solids. Combined these methods were highly effective in removing the filter cake, and in just a few cases there were visible remains left on the disc.

2.3.2 Disc mass

To determine the increase in mass, the ceramic discs were weighed at different stages in the test procedure. The most relevant of these measurements was the initial weight prior to the first permeability test, and the final weight after removing the filter cake. The disc mass was determined using Ohaus MB120 moisture analyzer, depicted in **Figure 6**, which heats the discs at 105 °C until the weight change is less than 1mg per 60 seconds.



Figure 6 - OHAUS MB120 moisture analyzer, used for removing moisture and determining disc mass.

2.3.3 Permeability

As mentioned previously, the invasion of different drilling fluid additives can cause damage to the formation in the form of reduced permeability. It is therefore interesting to investigate how the different samples affect the permeability of the discs through the fluid loss test. For each disc, the permeability to both water and air was measured before the fluid loss test, as well as after removing the filter cake. When measuring the permeability to air it is crucial to remove any moisture left in the disc, as it can inhibit flow through the disc. Therefore, the permeability to air was measured after determining the weight, as most of the moisture is removed from the disc in this process. The same equipment as described under filter cake removal was used for these measurements. However, two different cylinders were used, one for air and one for water permeability, to prevent any water remains to contaminate the disc and affect the measurements. After drying, the disc was installed in the acrylic cylinder and gas pressure was applied. Four sets of gas flow and air pressure measurements were recorded for each disc, as well as the air temperature in the outlet.

Air bubbles in the disc is a problem when measuring the permeability to water. They can affect the flow of fluid and thus the measured permeability. To counteract this the discs were submerged in water and put into a vacuum machine for 5 minutes, before being placed in an acrylic cylinder while submerged. The cylinder was then filled with room temperature water and mounted in the stand. A gas pressure of 25kPa was applied, and the pressure and flow readings were recorded at four different heights of the water column, as shown by the markings on the cylinder in **Figure 7**. The distance between each line is 1 cm, and as the height of the water column decreases, the hydrostatic pressure decreases as well. This affects the reading on the pressure sensor but is accounted for in the permeability calculations, which can be found in Appendix B.

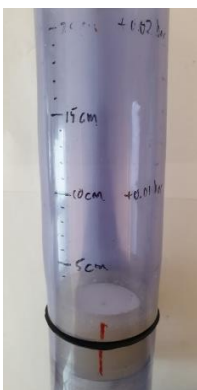


Figure 7 - Ceramic disc mounted in an acrylic cylinder

3 Results and Discussion

This chapter divided into four sections, where each addresses a different basis for comparison. Each section includes results for rheology, fluid loss, disc mass increase and permeability changes. Table 2 shows all the samples used in the following results, a short description of fluid content as well the median pore size of the disc used.

Table 2 - Overview of tests and samples.

Sample number	Description	Disc median pore size (μm)
1	Base fluid 1	20
2	Base fluid 1 plus bentonite	20
3	Base fluid 1 plus CaCO ₃	20
4	Base fluid 1 plus micronized barite	20
5	Base fluid 1 plus AURACOAT UF	20
6	Base fluid 1 plus bentonite and AURACOAT UF	20
7	Base fluid 1 plus CaCO ₃ and AURACOAT UF	20
8	Base fluid 1 plus micronized barite and AURACOAT UF	20
9	Base fluid 2 plus Polymer A and PAC	20
10	Base fluid 2 plus Polymer A and Polymer B	20
11	Base fluid 2 plus Polymer A and Starch	20
12	Base fluid 2 plus XC and PAC	20
13	Base fluid 2 plus XC and PAC	20
14	Base fluid 1 plus CaCO ₃	50
15	Base fluid 1 plus CaCO ₃ and AURACOAT UF	50

3.1 Effect of different solids

The scope of this section is to present the effect different solids has on rheology, fluid loss, particle invasion and permeability.

3.1.1 The effect of different solids on viscosity profiles

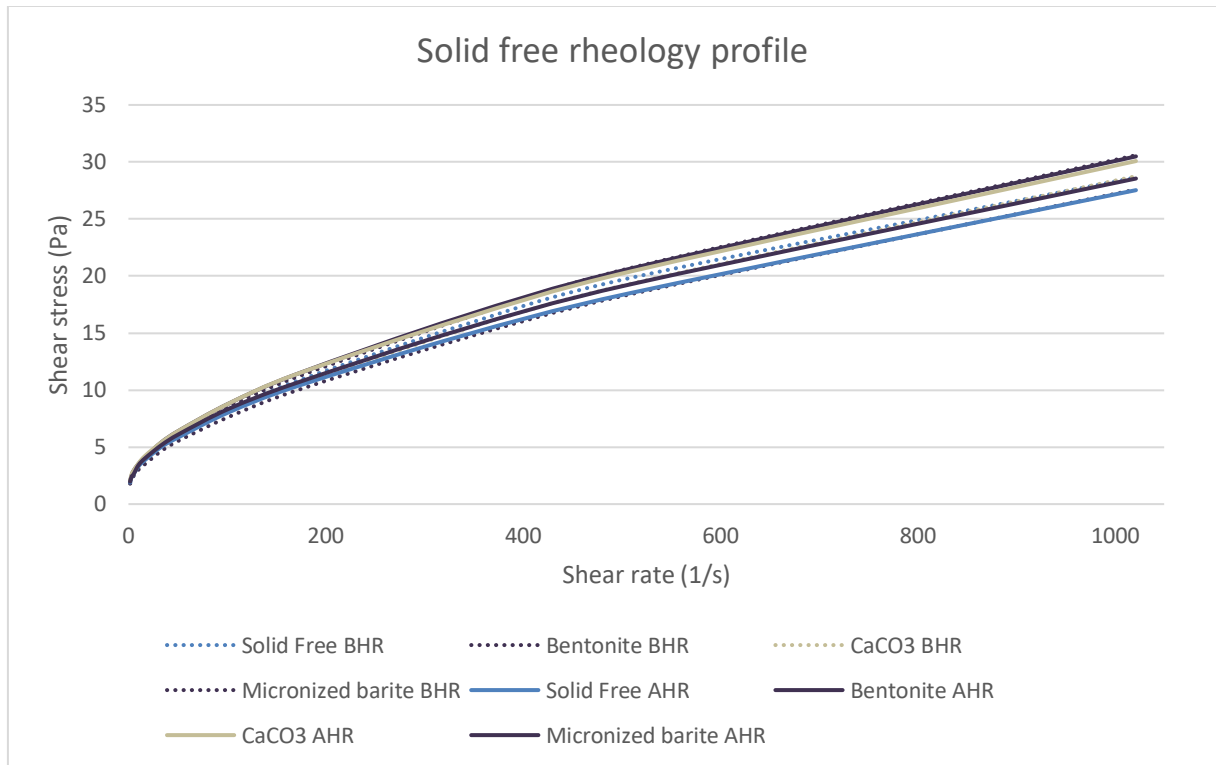


Figure 8 - Shear stress versus shear rate for solid free, bentonite, calcium carbonate and micronized barite samples.

All the samples used for this section contains the same polymers and only differ in solid content. Neither bentonite, calcium carbonate or micronized barite should notably affect the rheological properties of the fluid, and the viscosity profiles are thus expected to be similar. From **Figure 8**, some minor differences can be seen between the samples. The viscosity profiles for calcium carbonate and micronized barite are almost completely identical and has about 10 per cent higher shear stress compared to solid free. Bentonite is closer to the solid free, but also show an increase in shear stress of about 4 per cent. As the addition of solids slightly increase the shear stress, these fluids seem to have slightly higher viscosity. The particle size distribution is a possible explanation for the differences in viscosity profiles among solid containing fluids. The gap size between the bob and sleeve of the viscometer is 1.17mm, which is considerably larger than the particle size. However, the measured shear stress will increase as the particle size approaches the gap size. The differences before and after hot-rolling are minimal, indicating that the rheological properties remain intact.

3.1.2 The effect of different solids on fluid loss

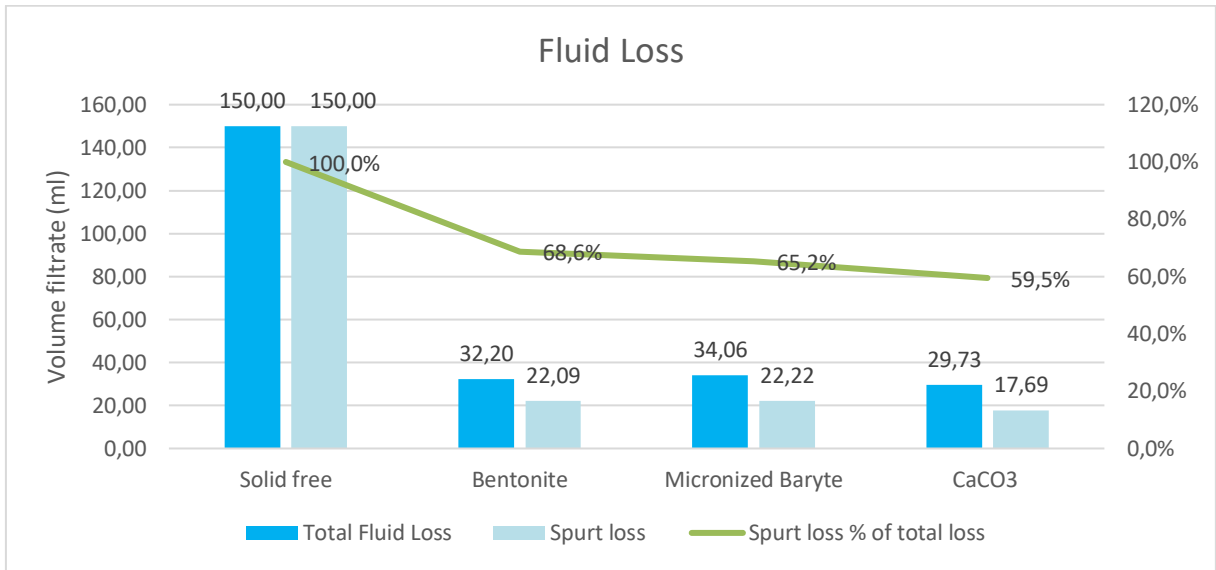


Figure 9 - Fluid loss results for solid free, bentonite micronized barite and calcium carbonate (Samples 1-4).

There were significant differences in measured fluid loss between the four samples. **Figure 9** shows the results from the HTHP fluid loss tests. For the solid free fluid there was a total loss, meaning that the whole cell volume was lost in the first few seconds of the test. This is not surprising considering there are no bridging materials such as solids or fibers added to the fluid, and the only additives that can help reduce fluid loss are the polymers. When adding bentonite, micronized barite or calcium carbonate to the fluid, there is a drastic improvement in sealing the disc and reducing fluid loss. The data shows that calcium carbonate have marginally lower total fluid loss compared to the other two. However, the difference comes from a lower spurt loss, and succeeding filtrate loss is in fact larger for calcium carbonate than bentonite and micronized barite. This can indicate that it takes less time for calcium carbonate to build a seal, but that does not mean the sealing capabilities over time will be stronger. With the addition of the solid particles in the fluid the sealing capabilities are increased, resulting in lower fluid loss.

3.1.3 The effect of different solids on disc mass

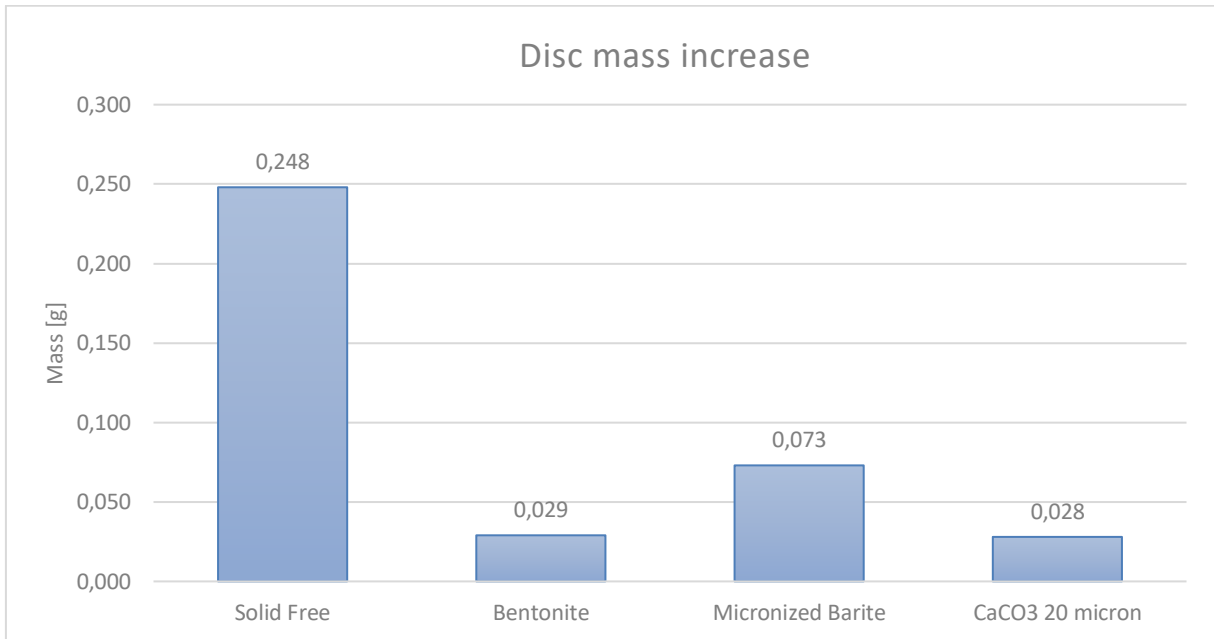


Figure 10 - Increase in mass of the ceramic discs used with solid free, bentonite, calcium carbonate and micronized barite.

The four fluids gave varying result regarding invasion of particles into the disc. Mass increase of the ceramic discs is shown in **Figure 10**. The solid free sample showed the highest increase in disc mass of all the samples with an increase of 248mg. This can be explained by the large fluid loss and poor sealing capabilities, resulting in polymers migrating into the disc. Xanthan gum consist of long molecular chains which causes it to easily get stuck inside the pores, and thus increasing mass of the disc. Bentonite and calcium carbonate both indicate relatively low invasion, with a mass increase of 29mg and 28mg respectively. Sample 4 containing micronized barite had a significantly higher mass increase compared to the other solids, with an increase of 73mg. It is important to note that the solids used have different densities. This means that even though barite gives a larger increase in disc mass, it does not necessarily indicate whether the invasion of particles and damage to the formation is larger. Additionally, this test does not provide any information regarding type of invasion, whether the migration consists of mostly solids or polymers. Looking only at changes in disc mass is therefore not a reliable measurement of formation damage. Adding solids to the fluid seems to improve the sealing capability and thus reduce the overall invasion of particles and polymers.

3.1.4 The effect of different solids on permeability

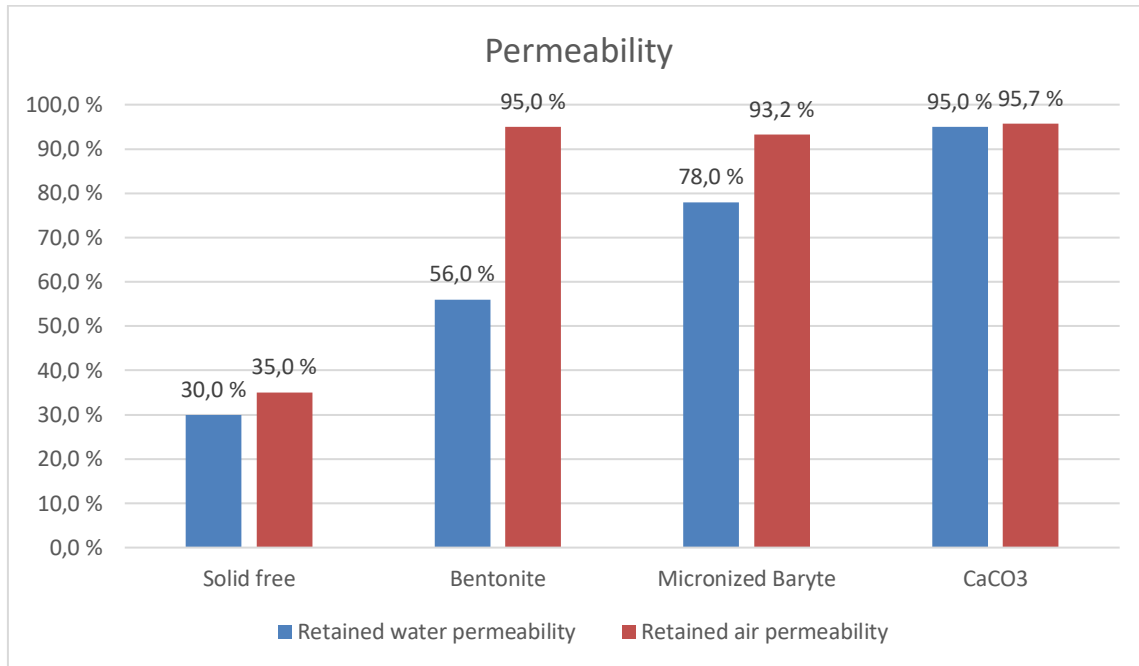


Figure 11 - Retained permeability to water and air for solid free, bentonite, micronized barite and calcium carbonate (Sample 1 to 4).

Changes in permeability can indicate formation damage. **Figure 11** presents how the permeability of the discs was affected by the different fluids. Retained permeability represents the final permeability of the disc as a percentage of the original permeability. The solid free fluid caused a drastic reduction in permeability of the disc, which retained 30 per cent of its original permeability to water and 35 per cent to air. This is most likely due to a combination of high fluid loss and disc mass increase, indicating high polymer content in the disc, which causes plugging of the pores. The retained permeability seems to always be higher for air than for water. The capillary effect can be a possible explanation for this. As the pores get partially plugged and the pore size decreases, the fluid flow will be affected more than the air flow. The difference between water and air permeability is most significant for bentonite. A reason for this can be its high swelling capacity, causing remaining clay particles to swell and clog pores during the final water permeability measurement. Micronized barite and calcium carbonate show similar results regarding air permeability but differ in retained water permeability. This can be explained by the higher disc mass increase for micronized barite, as well as the natural bridging properties of the calcium carbonate. Adding solids to the fluid seems to reduce the invasion, improving the retained permeability and reducing formation damage. Among the solids tested, calcium carbonate shows the best performance.

3.2 Effect of adding fibers

In this section the effects of adding a fiber based lost circulation material will be evaluated. The results presented consists of samples 1-8, where samples 5-8 uses the same recipes as 1-4, but with the addition of AURACOAT UF.

3.2.1 The effect of adding fibers on viscosity profiles

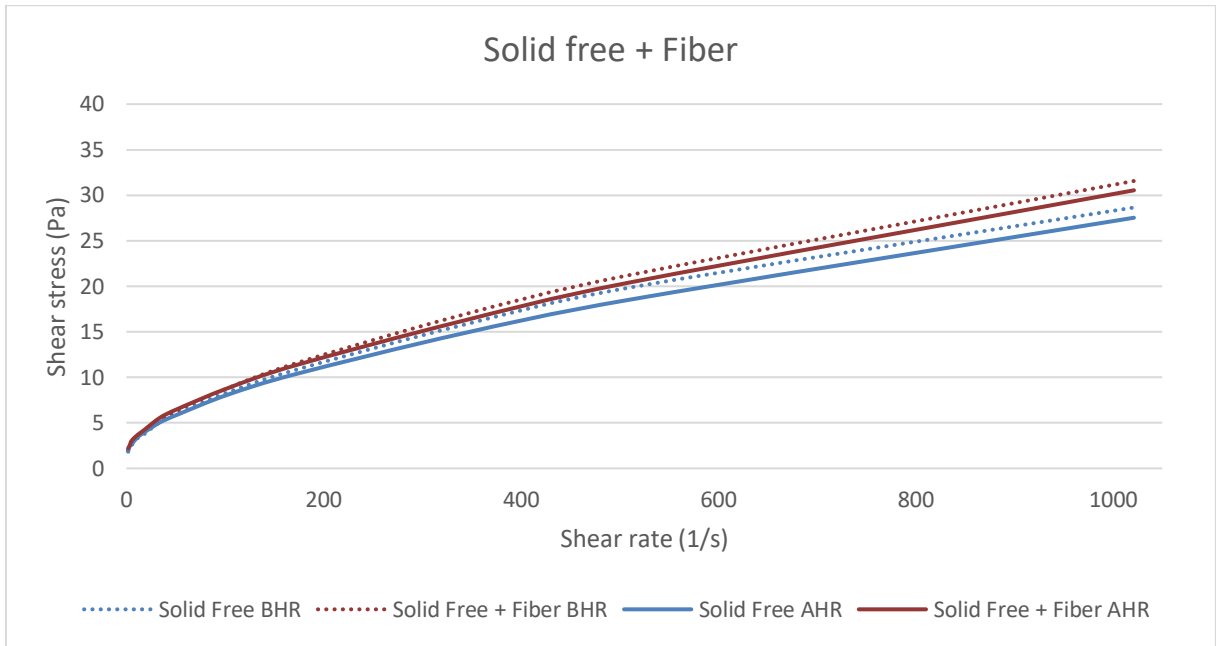


Figure 12 - Shear stress versus shear rate for solid free fluid, with and without fiber (Sample 1 and 5).

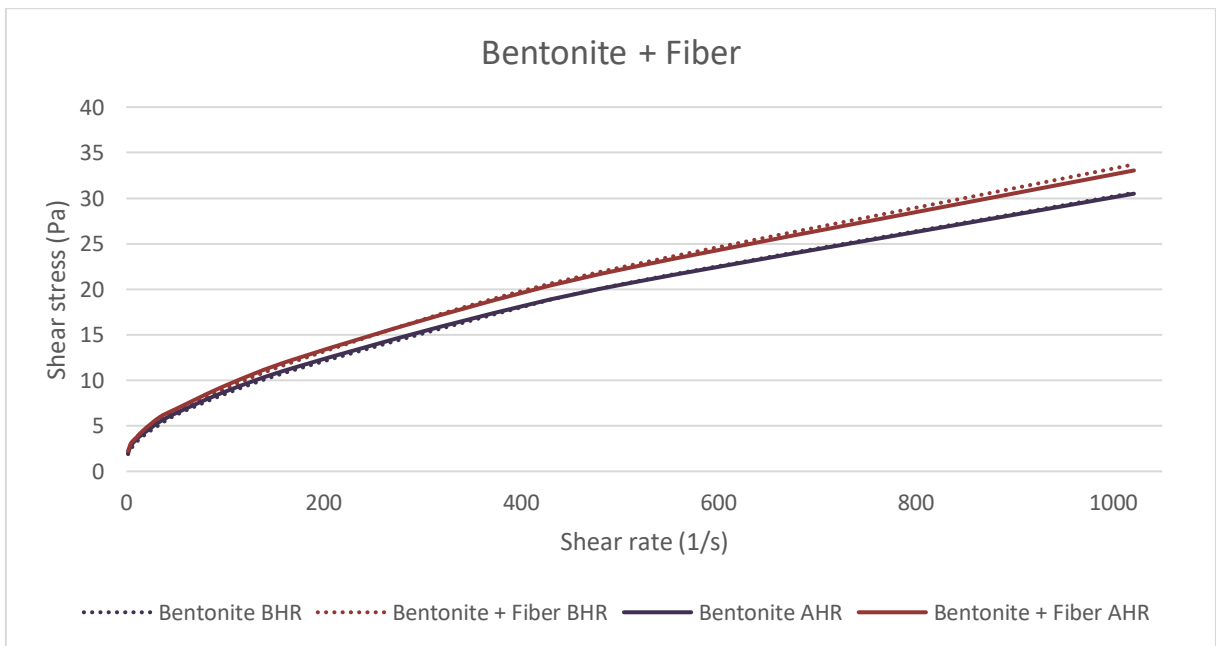


Figure 13 - Shear stress versus shear rate for bentonite fluid, with and without fiber (Sample 2 and 6).

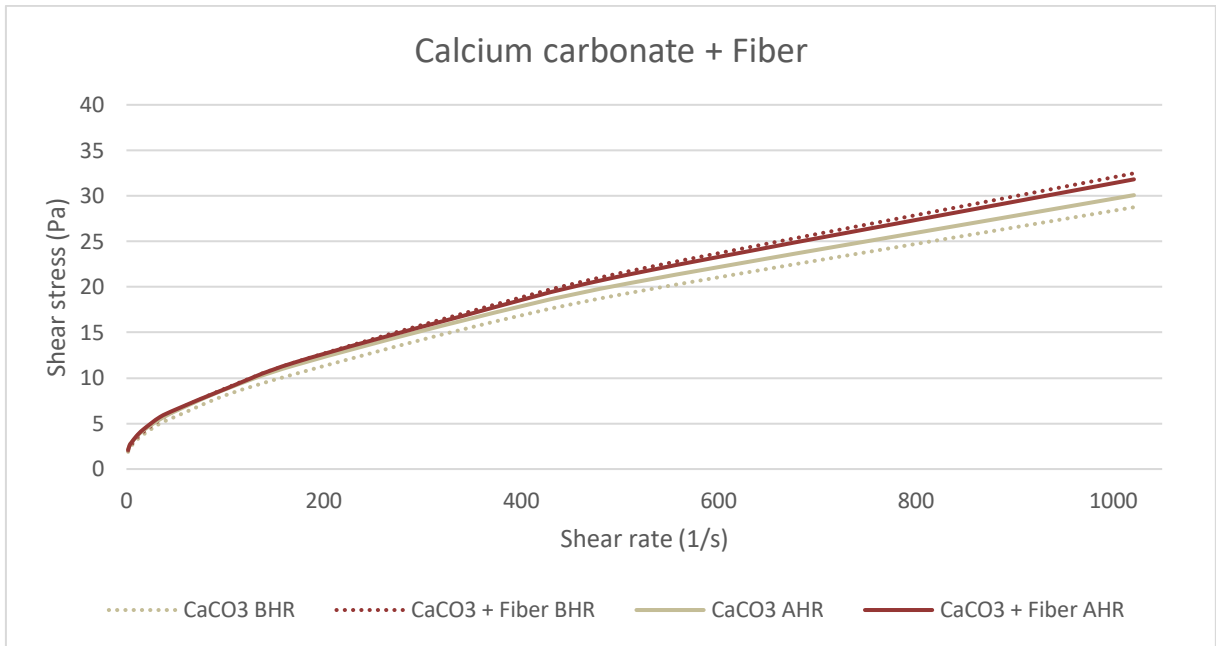


Figure 14 - Shear stress versus shear rate for calcium carbonate fluid, with and without fiber (Sample 3 and 7).

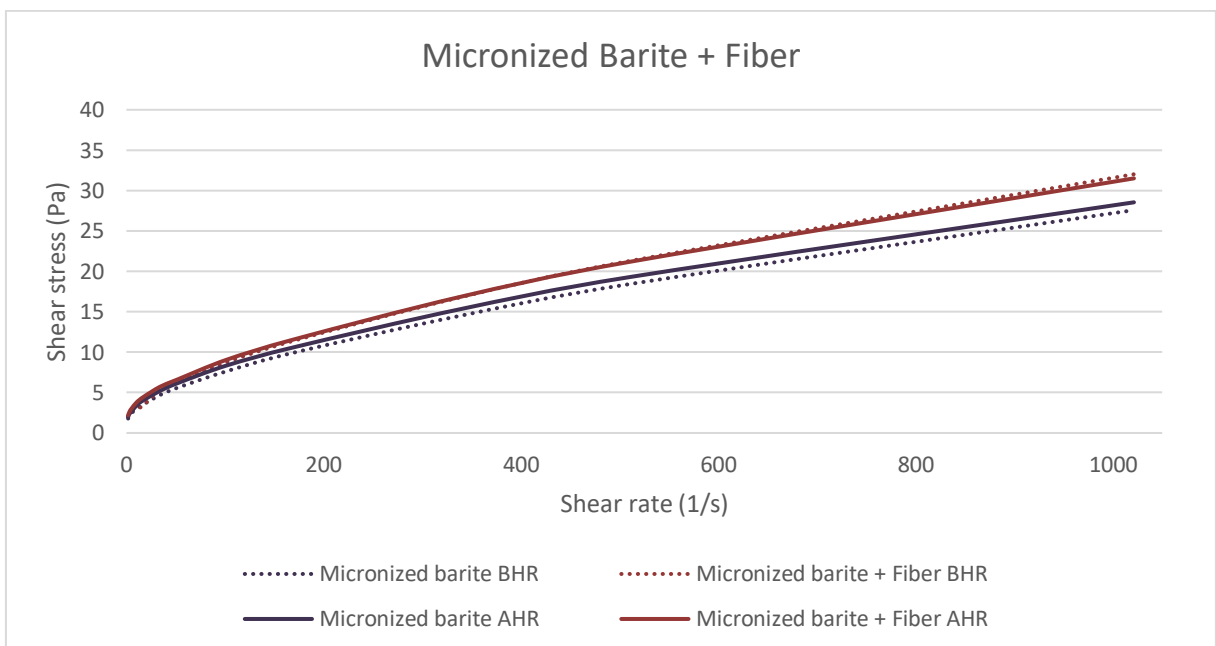


Figure 15 - Shear stress versus shear rate for micronized barite fluid, with and without fiber (Sample 4 and 8).

Fibers are primarily added to drilling fluids to increase the sealing capabilities and prevent lost circulation and should have little effect on the rheology. **Figures 12 through 15** shows the effect fibers has on the viscosity profiles. The addition of fiber seems to increase the shear stress by approximately 10 per cent for all shear rates, indicating an increased viscosity. A possible reason is that a portion of the fluid is bound in the fiber, effectively reducing water concentration, and thus increasing the viscosity. The irregular shape of the fibers can also affect the measurements. They are often much longer in one direction and not as rounded as solid particles. Rotation of these longer fibers can exert additional pressure on the bob in the

viscometer, resulting in higher shear stress. Hot-rolling marginally reduces the viscosity profiles for all samples containing fiber.

3.2.2 The effect of adding fibers on fluid Loss

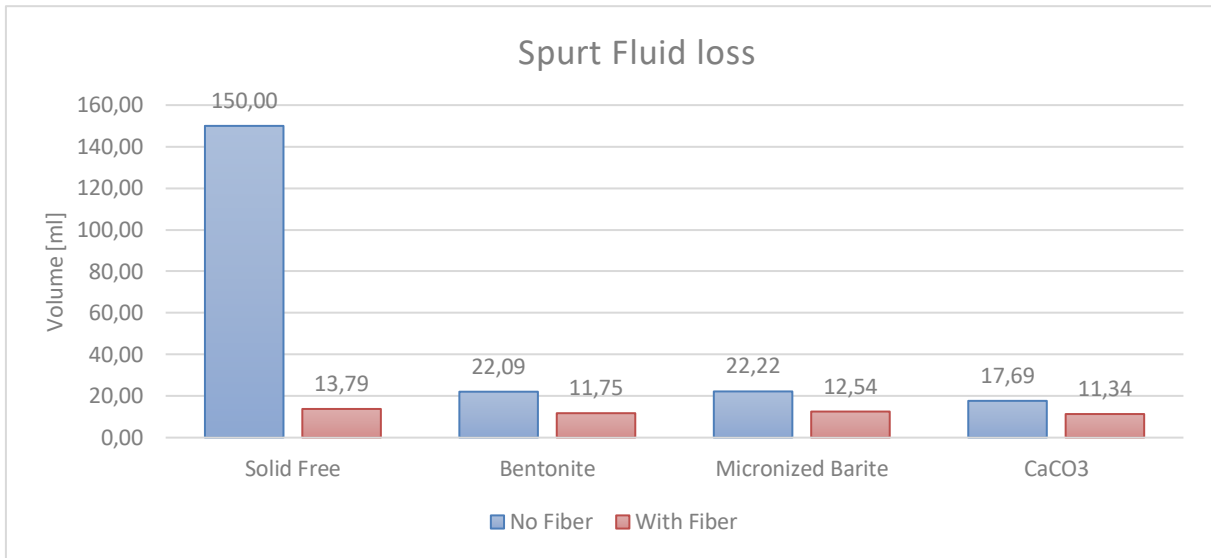


Figure 16 - Spurt fluid loss for solid free, bentonite, micronized barite and calcium carbonate, with and without fiber (Sample 1-8).

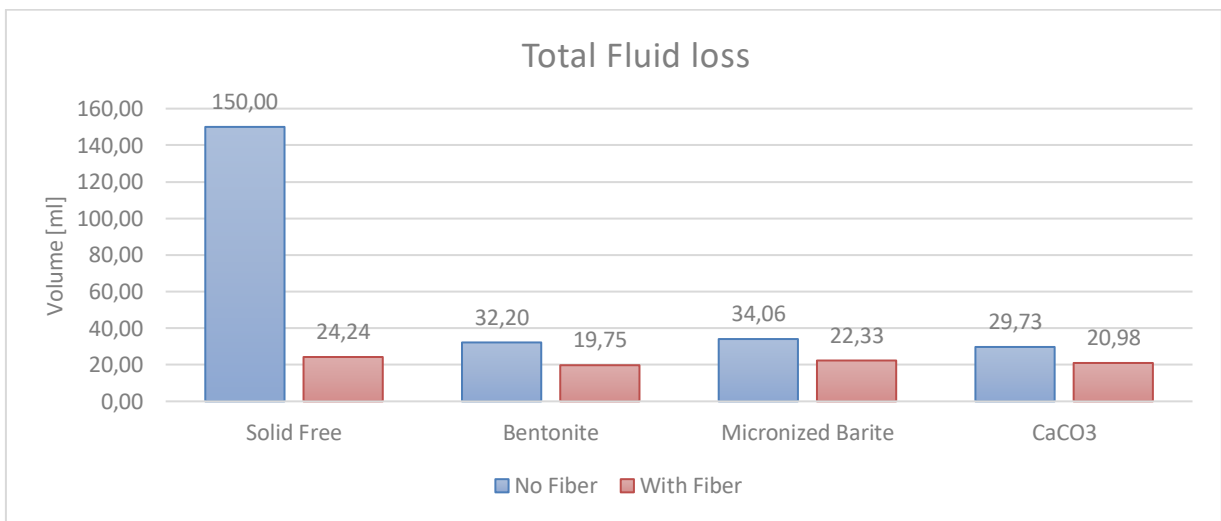


Figure 17 - Total fluid loss for solid free, bentonite, micronized barite and calcium carbonate, with and without fiber (Sample 1-8).

With the addition of fibers, both total fluid loss and spurt loss was reduced for all samples. **Figures 16 and 17** shows how adding fibers affected the filtrate volume for the different fluids. The blue columns represent Sample 1-4, while the red columns represent Sample 5-8 containing fiber. The effect was most significant in the solid free sample, which went total loss to having lower fluid loss than the solids samples without fibers. Adding fiber to the bentonite sample reduced the total filtrate volume by 39 per cent, and the spurt loss by 47 per cent. For micronized

barite the addition of fiber reduced the total fluid loss by 34 per cent, and spurt by 44 per cent. For calcium carbonate the total filtrate volume was reduced by 29 per cent, and spurt loss by 36 per cent when adding fibers. Interestingly, the reduction in spurt loss is noticeably higher than the total fluid loss reduction. Indicate that the fibers improve not only the sealing capabilities of the fluid but also the sealing rate.

3.2.3 The effect of adding fibers on disc mass

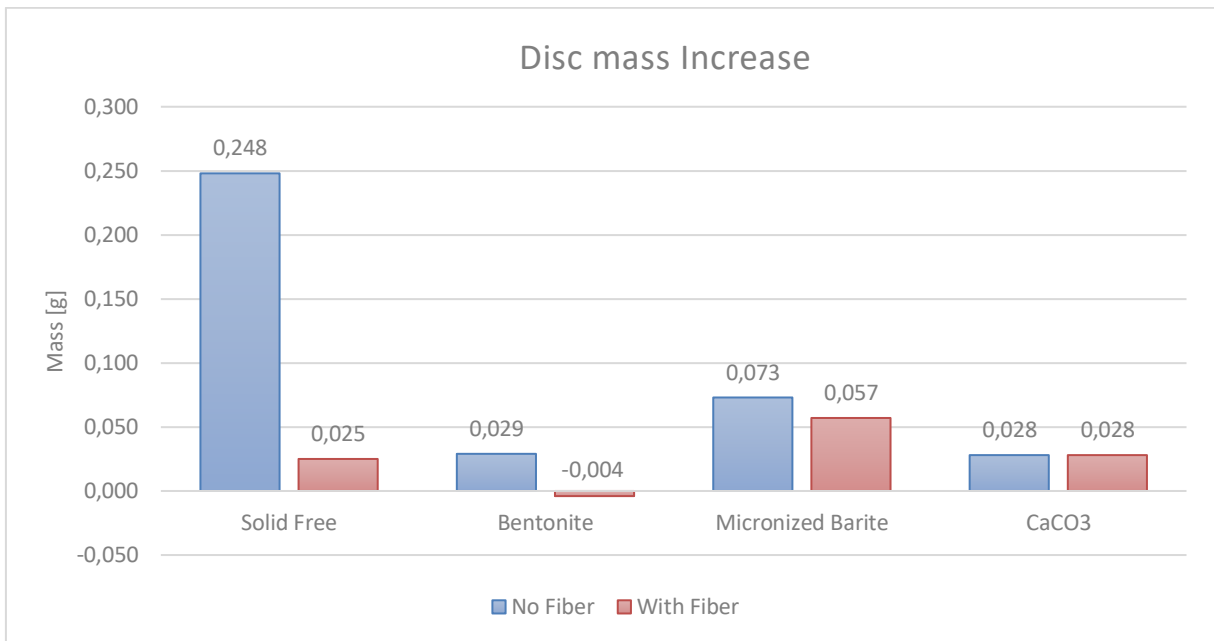


Figure 18 - Increase in disc mass for solid free, bentonite, micronized barite and calcium carbonate, with and without fiber, (Sample 1-8).

The addition of fibers to the samples had a significant effect on disc mass. **Figure 18** shows disc mass increase with and without fiber. The effect was most noticeable with the solid free sample, which went from having the largest mass increase of 248mg to only 25mg, meaning a reduction of almost 90%. This indicates that the fibers drastically improve the sealing capability of the drilling fluid and helps reduce fluid loss and invasion of polymers. It is unclear why the disc used for sample 6, containing bentonite, showed a reduction in disc mass. A reason could be inaccurate measurements of the initial weight, or that the disc contained fines which were flushed out during the tests. Looking at the results with the other solids, the addition of fiber had a good effect with micronized barite, reducing the invasion by 22 per cent. With calcium carbonate, there was no change in the mass increase of the disc. There was some uncertainty regarding the breaker fluid used on micronized barite with fiber and calcium carbonate with fiber. It is believed that it might not have been mixed properly, resulting in reduced effectiveness in removing the filter cake. It is therefore likely that the reported disc

mass increase for these samples is overproportioned. Generally, it seems like adding fibers to the drilling fluid helps reduce invasion.

3.2.4 The effect of adding fibers on permeability

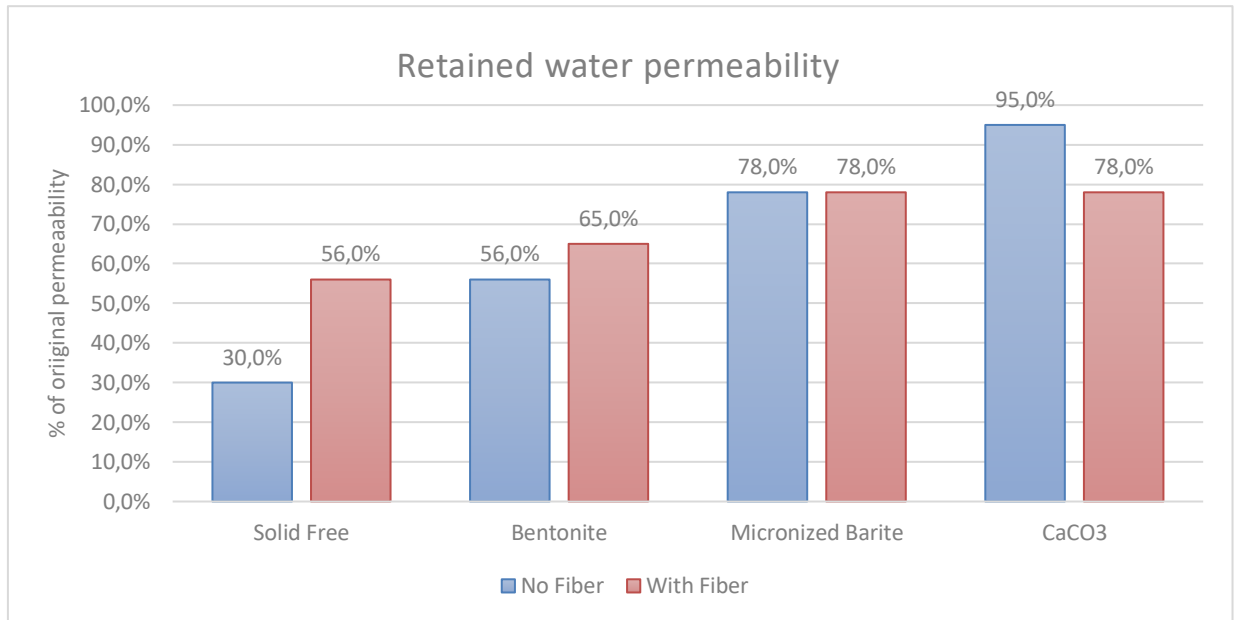


Figure 19 - Retained permeability to water for solid free, bentonite, micronized barite and calcium carbonate, with and without fiber (Sample 1 to 8).

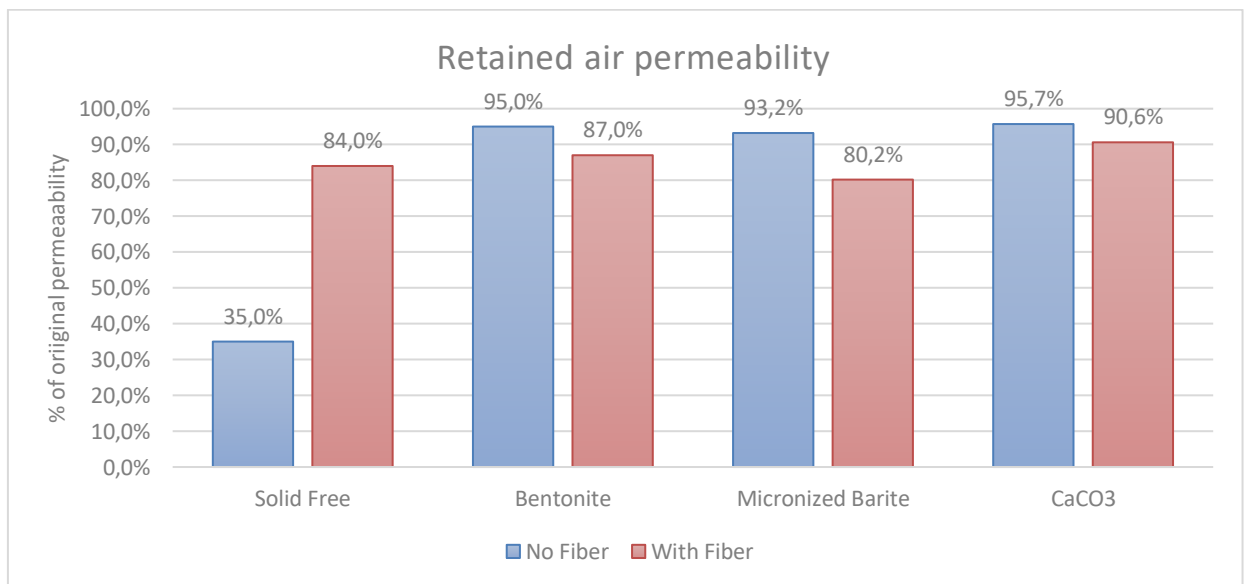


Figure 20 - Retained permeability to air for solid free, bentonite, micronized barite and calcium carbonate, with and without fiber (Sample 1 to 8).

The addition of fibers to the samples had varying results regarding changes in permeability. **Figure 19** shows how the presence of fibers in the drilling fluid affects the retained water permeability. There was a significant improvement for the solid free fluid, increasing retained water permeability from 30 to 56 per cent. The effect with bentonite was

also significant, increasing the permeability by 9 percentage points. With micronized barite, the fiber showed no effect, and with calcium carbonate, the permeability to water was reduced by 17 per cent. This can be related to the uncertainty regarding the breaker fluid, as discussed in the previous section.

Looking at results for retained permeability to air, shown in **Figure 20**, the addition of fibers had some unexpected results. While the solid free fluid increased 49 percentage points, the retained air permeability was reduced for all fluids containing solids. It is unclear why the introduction of fibers could cause a reduction. One explanation is related to the drying process, which involves heating the discs at 105 °C for 30-60 minutes, depending on fluid content. This should have little effect on the solids but could cause a reaction between the polymers and fiber.

3.3 Effect of different polymers

In this section the effect of using different polymer combinations will be evaluated.

3.3.1 The effect of using different polymers on viscosity profiles

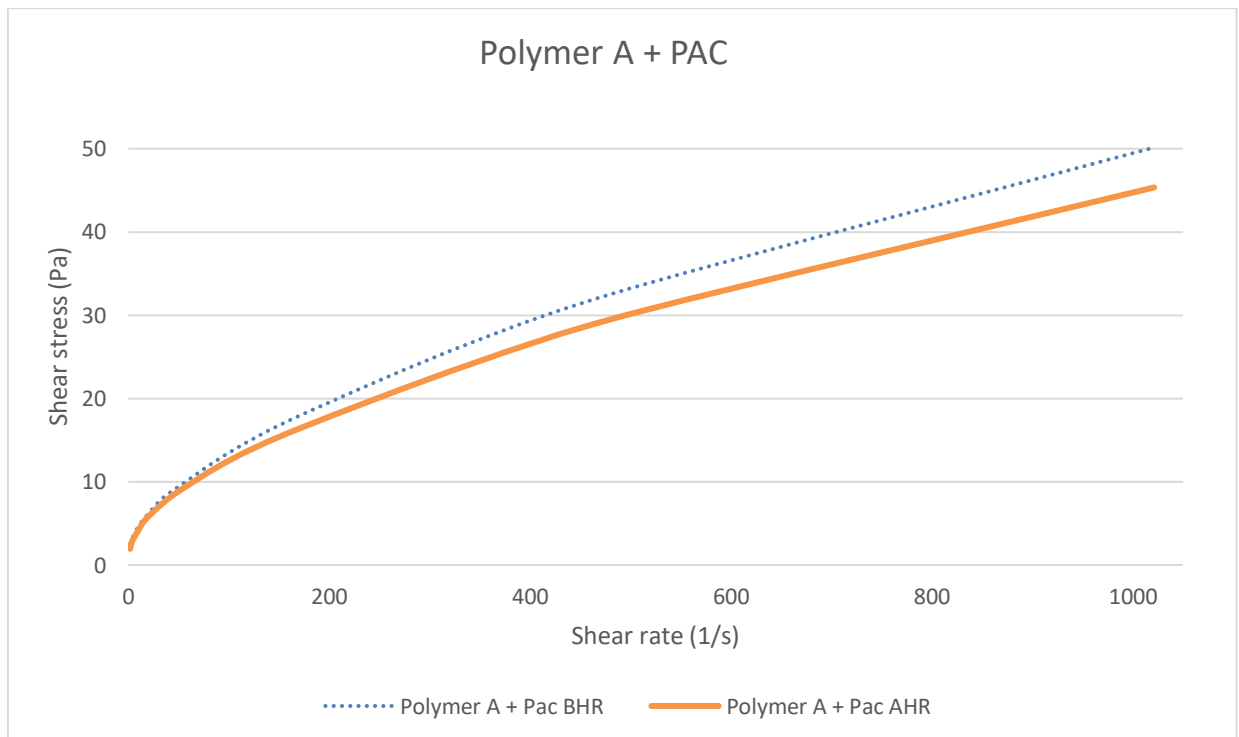


Figure 21 - Shear stress versus shear rate for Polymer A and PAC combination (Sample 9).

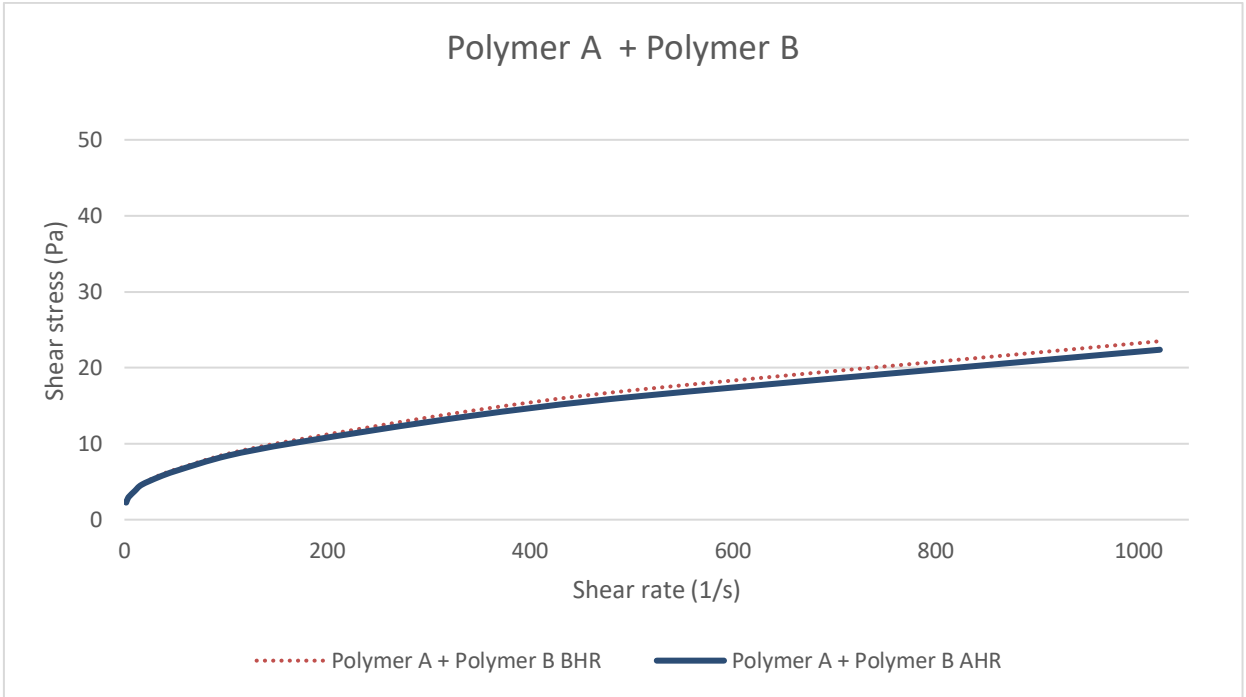


Figure 22 - Shear stress versus shear rate for Polymer A and Polymer B combination (Sample 10).

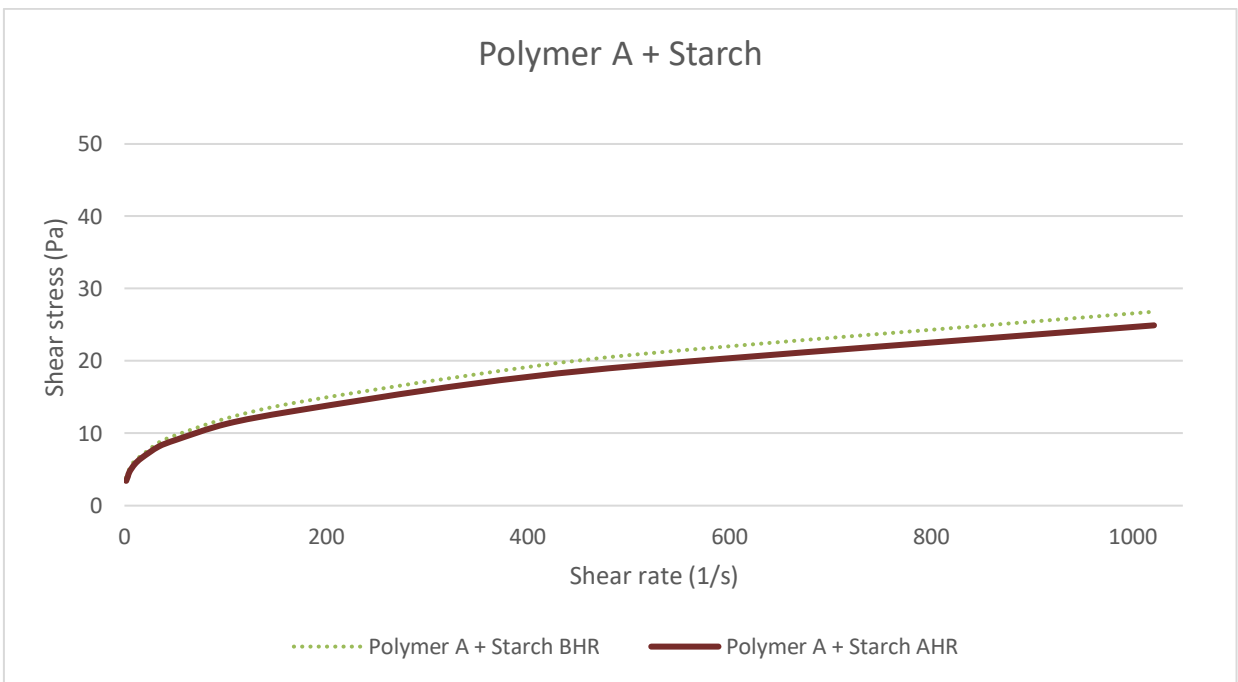


Figure 23 - Shear stress versus shear rate for Polymer A and Starch combination (Sample 11).

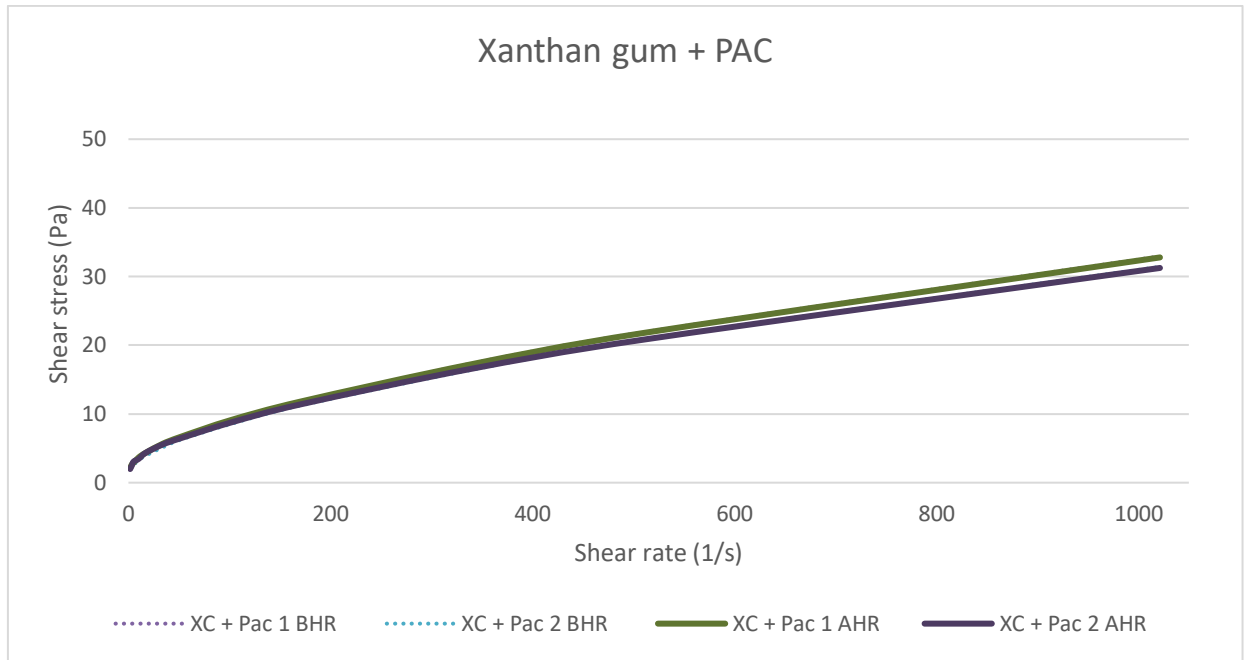


Figure 24 - Shear stress versus shear rate for Xanthan gum and PAC combination (Sample 12 and 13).

One of the main functionalities of polymers is to provide viscosity to the drilling fluid. The fluids presented in this section contains different types and concentration of polymers. It is therefore expected that the differences in viscosity profiles will be much more prevalent compared to the effect of different solids and fiber. Polymer A is a modified starch designed to increase viscosity and reduce fluid loss. Polymer B is a modified starch and cellulose, designed to give viscosity at low shear rates, while providing extreme shear thinning behavior. **Figures 21 through 24** presents the viscosity profiles of the different fluids. The combination of polymer A and PAC provides the highest shear stress for different shear rates, which is not surprising considering both the polymers provides viscosity. This combination also shows a noticeable change after hot-rolling, indicating that the rheological properties might dissipate during circulation. Polymer A and polymer B combination has the lowest viscosity profile and provides distinct shear thinning behavior. Polymer A combined with starch is very similar to the previous combination but provides slightly higher shear stress for low shear rates and shows the most shear thinning behavior among the different polymer fluids. Xanthan gum and PAC has the most linear viscosity profile, which means it is not as shear thinning.

3.3.2 The effect of using different polymers on fluid loss

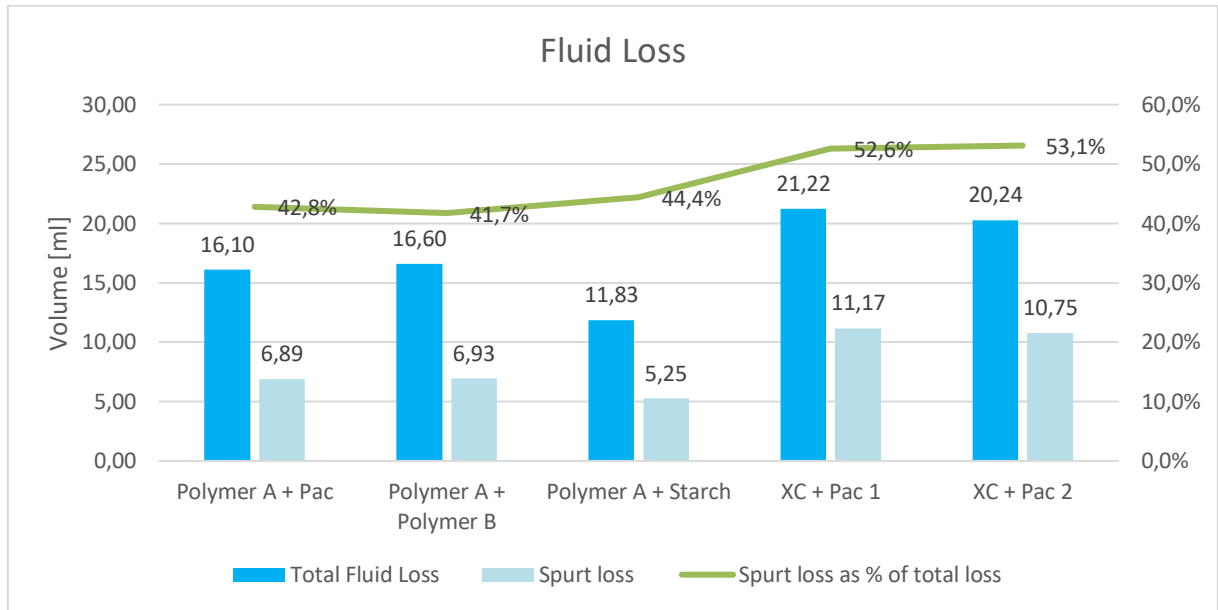


Figure 25 - All fluid loss results for the different polymer combinations (Sample 9 to 13).

One of the properties of polymers is to reduce fluid loss, and it is therefore expected that fluid loss will vary for the different polymer combinations. **Figure 25** show the filtrate volumes from the HTHP tests for the different fluids presented in this section. While the combinations of Polymer A with PAC (Sample 9) and Polymer A with Polymer B (Sample 10) had significantly different viscosity profiles, the fluid loss was almost identical. This may indicate that 5g of PAC provides equal sealing capabilities as 3g of Polymer B. Combining Polymer A with starch resulted in the smallest filtrate volume of all the HTHP fluid loss tests. This could mean that starch provides superior fluid loss reduction. However, the concentration of starch is higher than the concentration of PAC and Polymer B. The spurt loss as per cent of total loss is noticeably lower for the samples containing Polymer A, which indicate a higher sealing rate compared to xanthan gum and PAC.

Both the fluids containing xanthan gum and PAC uses the same recipe and unsurprisingly give very similar fluid loss results. An interesting thing to note is that the original permeability of the disc used for Sample 13 was 20 per cent higher than the one used for Sample 12. This is the opposite of what is expected, as it is natural to believe that higher permeability would lead to higher fluid loss. Some possible testing related factors that can explain these includes inaccuracies in mud preparation, fluid loss procedure or permeability measurements.

3.3.3 The effect of using different polymers on disc mass

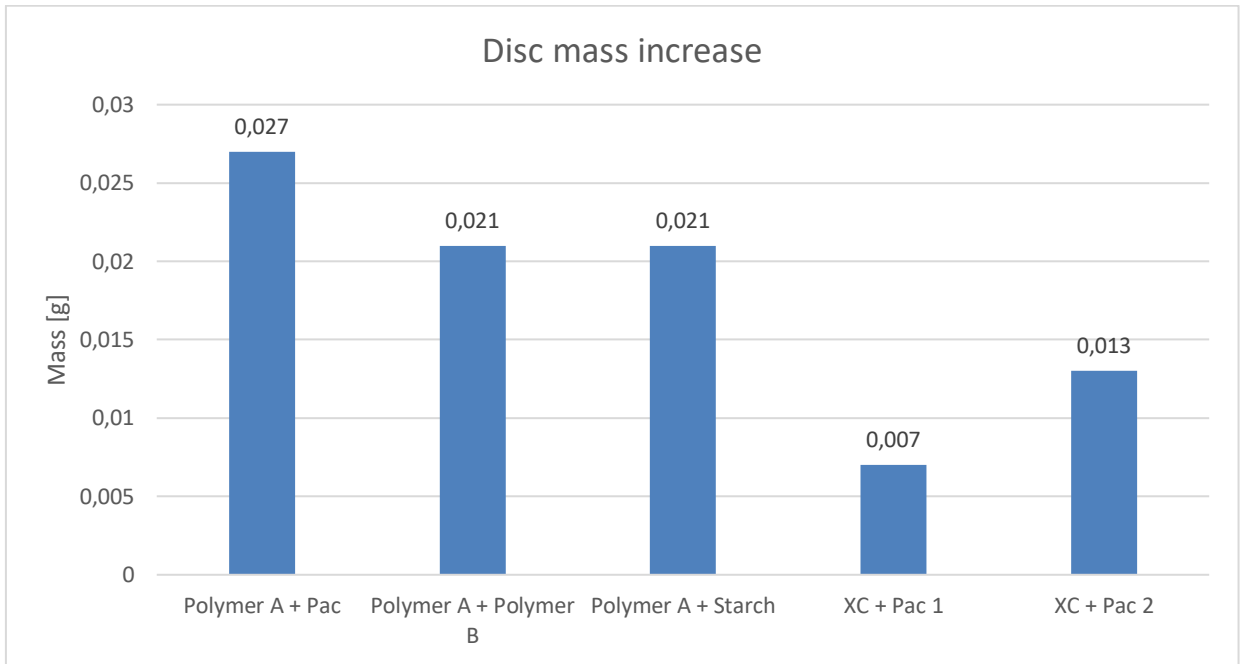


Figure 26 - Disc mass increase using different polymer combinations (Samples 9-13).

The different fluids had small but noticeable effects on the disc mass. **Figure 26** show the increase in mass of the discs used for Samples 9-13. The variations in disc mass were much smaller for the different polymer combinations than the different solids, ranging from 7mg for xanthan gum with PAC, to 27mg for Polymer A with PAC. This is partly because these fluids contain both calcium carbonate and fiber, providing great sealing capabilities. The increase in disc mass is significantly higher for the combinations with Polymer A than for xanthan gum and PAC. This indicates that xanthan gum and PAC provides superior properties in reducing invasion. The fluid loss data suggested that combinations of Polymer A gave the lower fluid loss, and a higher sealing rate. This indicates that there is no clear connection between fluid loss and formation damage, which is consistent with the results from Green et al. [6].

3.3.4 The effect of using different polymers on permeability

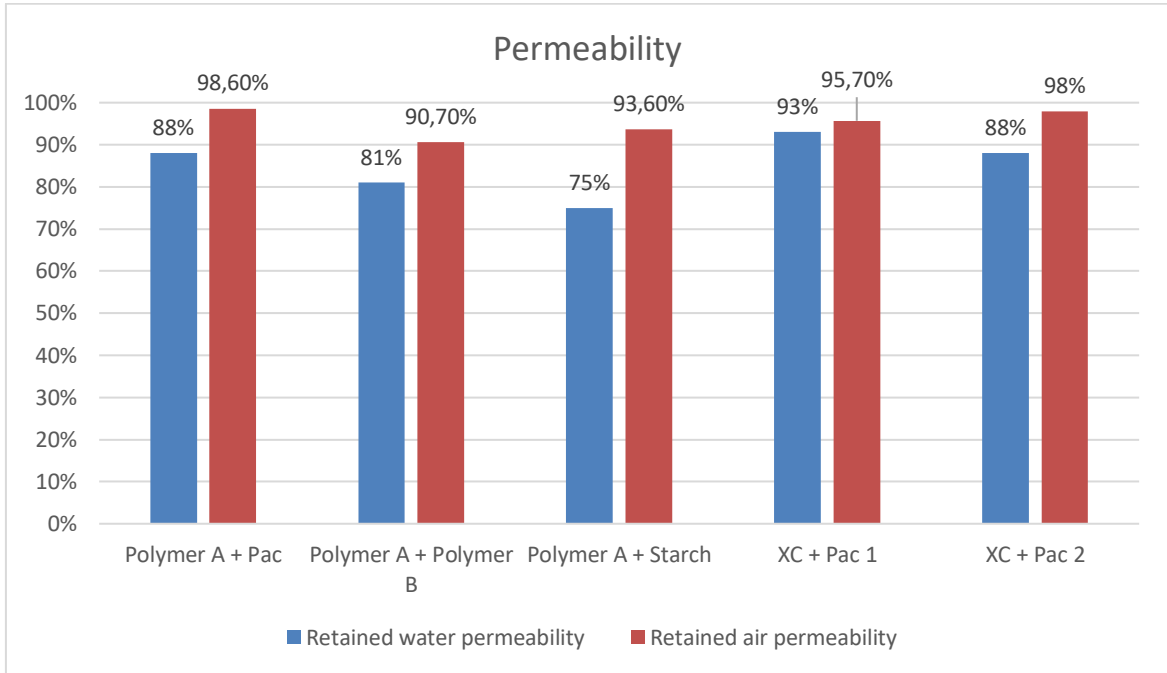


Figure 27 - Retained permeability to air and water using different polymer combinations (Samples 9-13).

Different polymers also affect the permeability of the discs. The retained permeability results are given in **Figure 27**. Xanthan gum and PAC seems to give marginally higher retained water permeability than the combinations of Polymer A. This may indicate that lower disc mass results in higher permeability, and thus less damage to the formation.

3.4 Different concentration of CaCO₃ and different median pore sizes

The effect of adding fibers to calcium carbonate has already been evaluated. However, it is interesting to see if anything changes when the concentration of calcium carbonate increases, and when the median pore size is larger.

3.4.1 The effect of increasing concentration of CaCO₃ on viscosity profiles

The rheology measurements are unrelated to the median pore size of the disc; however, the concentration of calcium carbonate is doubled for the samples used on the 50 μ m disc, which can affect the rheological properties of the fluid. **Figure 28** shows the viscosity profiles for different concentration of calcium carbonate without fiber. There does seem to be any noticeable differences. Looking at **Figure 29**, the addition of fiber increases the share stress by about 4 to 5 per cent for high shear rates, indicating slightly higher viscosity.

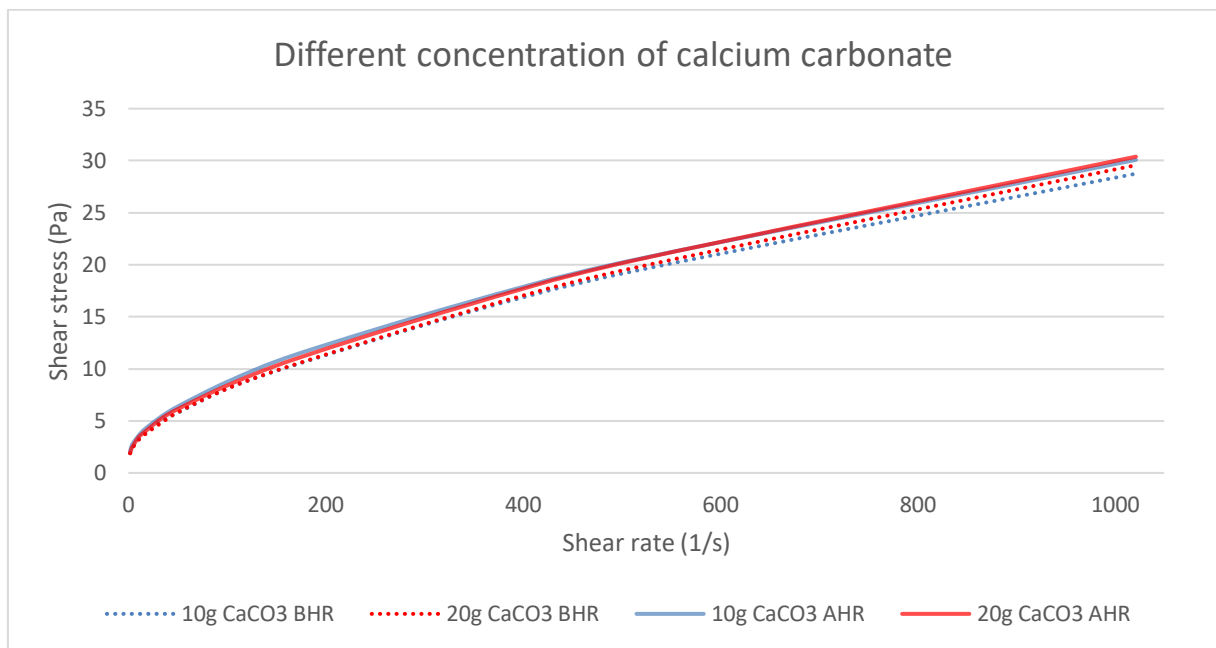


Figure 28 - Shear stress versus shear rate for fluids with different concentrations of calcium carbonate (Sample 3 and 14)

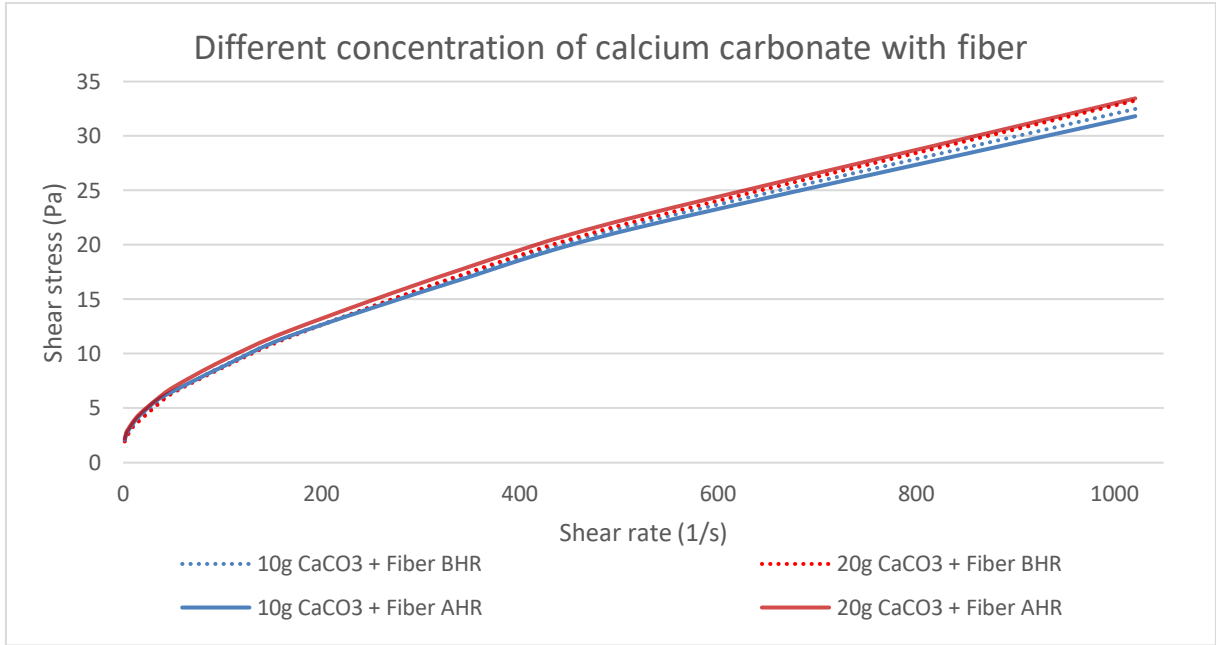


Figure 29 - Shear stress versus shear rate for fluids with fiber and different concentrations of calcium carbonate (Sample 3 and 14)

3.4.2 The effect of increasing concentration of CaCO₃ and median pore size on fluid loss

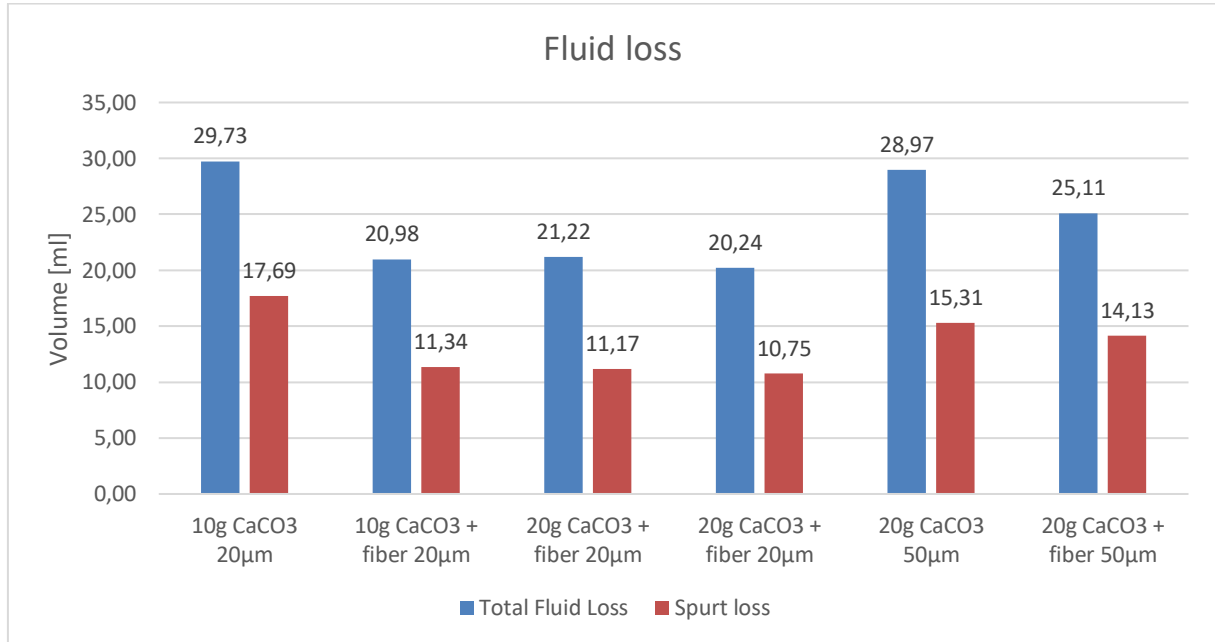


Figure 30 - Fluid loss results different concentration of calcium carbonate, and different median pore sizes. (Samples 3, 7, 12-15)

Figure 30 shows the fluid loss results with different concentration of calcium carbonate and different median pore sizes. For a 20μm disc, an increased concentration of calcium carbonate does not seem to affect the fluid loss if there are fiber added to the fluid. Comparing 20g CaCO₃ on a 50μm disc to 10g CaCO₃ on a 20μm disc the fluid loss is marginally lower with the 50μm. When comparing the same fluids, but with the addition of fiber, the fluid loss is noticeably higher with the 50μm disc, with an increase of 4.13ml. Although there is no data for 10g CaCO₃ on a 50μm, this can indicate that a higher concentration of calcium carbonate helps reduce fluid loss when no fiber is added, as fluid loss is expected to increase with larger pore sizes. Looking at 20g CaCO₃ with fiber on a 20μm disc versus a 50μm disc the total fluid loss is increased by approximately 4.5ml, or 18 per cent for the 50μm disc. This can be explained by the particle size distribution of the calcium carbonate, which only consists of particles smaller than 53μm. This means that most of the particles are smaller than the median pore size, and thus the sealing capabilities are expected to be reduced. Generally, it seems like increasing the concentration of calcium carbonate from 10g to 20g can reduce fluid loss when there are no fibers added to the fluid. The fluid loss also seems to increase when the median pore size of the disc increases.

3.4.3 The effect of increasing concentration of CaCO₃ and median pore size on disc mass

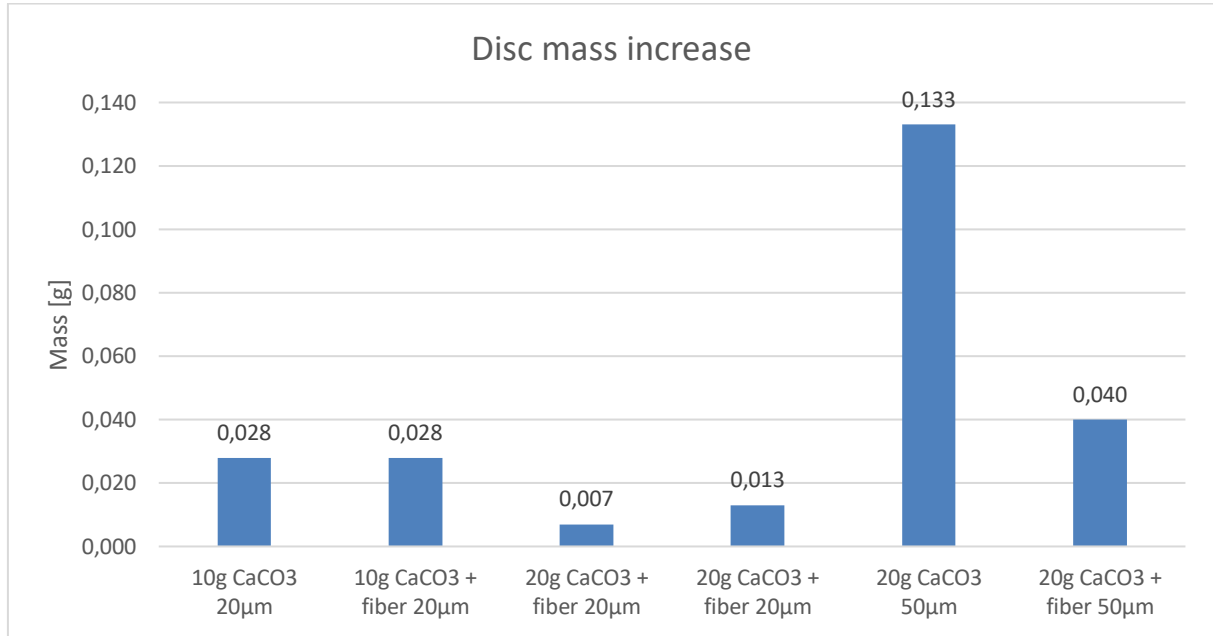


Figure 31 - Increases in disc mass for different concentration of calcium carbonate, and different median pore sizes. (Samples 3, 7, 12-15)

Figure 31 shows the results of how disc mass was affected by the different fluids. When fiber is present in the drilling fluid it seems like doubling the concentration of calcium carbonate reduces the change in disc mass from 28mg to 7-13mg. This may indicate that a higher concentration of calcium carbonate helps reduce the invasion of polymers and solids. The 50µm disc used with 20g CaCO₃ increased disc mass by 133mg, while the 20µm with 10g CaCO₃ only increased by 28mg. Even though the concentration of calcium carbonate is doubled, the mass increase is almost five times higher, which indicates that as the median pore size exceeds the particle size, the invasion is greatly increased. Comparing 20g CaCO₃ with fibers on a 50µm to a 20µm the change in disc mass is still noticeable greater for the 50µm disc, with an increase of 40mg. However, this is significantly lower than without fibers in the fluid. This means that even though the median particle size of calcium carbonate is lower than the median pore size, adding fiber to the drilling fluid can drastically reduce the invasion.

3.4.4 The effect of increasing concentration of CaCO₃ and median pore size on permeability

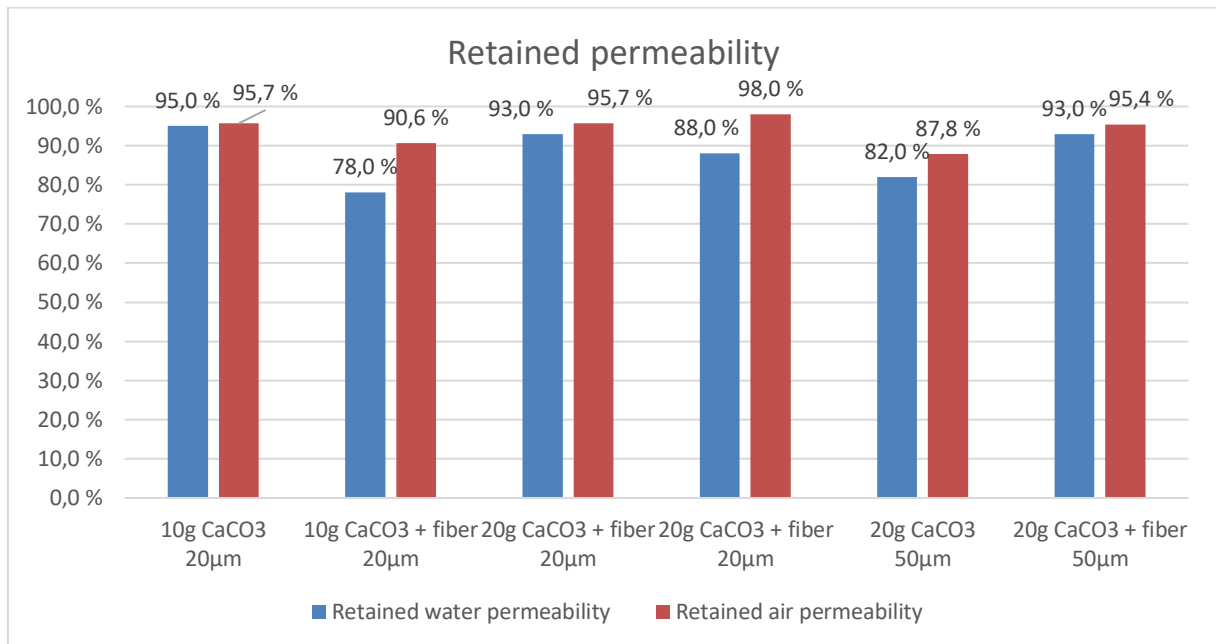


Figure 32 - Retained permeability to water and air for different concentration of calcium carbonate, and different median pore sizes. (Samples 3, 7, 12-15)

Changing the concentrations of calcium carbonate can also affect the permeability of the disc. Using the results presented in **Figure 32**, the effect on retained permeability can be evaluated. Looking at the 20μm discs and a fluid containing fiber, a doubling of the calcium carbonate concentration increased the retained water permeability from 78 per cent to 88-93 per cent. The retained permeability to air was also increased by about 5-8 percentage points. This suggests that increasing the concentration of calcium carbonate can improve the sealing capabilities, and thus reduce invasion and formation damage.

Comparing 10g CaCO₃ on a 20μm disc to 20g CaCO₃ on a 50μm disc, the retained permeability to water was reduced by about 14 per cent, and the retained permeability to air was reduced by approximately 8 per cent. With the addition of fiber and a calcium carbonate content of 20g for both fluids, there is no definite difference in the retained permeability of the discs. This suggests that the increased pore size can lower permeability if there is no fiber in the drilling fluid.

4 Conclusion

Although the testing conditions may deviate from the actual conditions in a well, measuring changes in mass and permeability of the ceramic discs gives a better comprehension of how different additives may cause damage to the formation. Based on the results the following conclusions were made:

- The solid free fluid was ineffective in preventing loss of fluid to the formation, which resulted in significant invasion and permeability alterations.
- The addition of solids to the drilling fluid improved the sealing capability, and significantly reduced fluid loss and formation damage. Among the solids, calcium carbonate showed the best performance.
- Adding fiber to the solid free fluid had a greater effect in reducing fluid loss and mass increase of the disc, compared to the addition of solids. However, it was less effective in preventing changes to the permeability.
- Combining the use of fibers, polymers and solids seem to be the most effective way of reducing fluid loss and damage to the formation.
- The results suggest no clear relationship between fluid loss and changes in disc mass or permeability. This is especially apparent when comparing different polymer combinations.
- A larger pore size results in greater invasion but does not necessarily affect fluid loss and permeability.
- There seem to be a negative correlation between an increase in disc mass and retained water permeability.
- Invasion seems to affect the permeability to water more than the permeability to air.

5 References

1. Zhang, J., Yin, SX., “Fracture gradient prediction: an overview and an improved method”, *Pet. Sci.* **14**, 720–730, 2017. DOI: [10.1007/s12182-017-0182-1](https://doi.org/10.1007/s12182-017-0182-1)
2. Alsaba, M., Nygaard, R., Saasen, A., Nes, O.M., “Lost Circulation Materials Capability of Sealing Wide Fractures”, SPE-170285-MS, SPE Deepwater Drilling and Completions Conference, Galveston, TX, USA, 2014. DOI: [10.2118/170285-MS](https://doi.org/10.2118/170285-MS)
3. Civan, F., Reservoir Formation Damage 2020, Gulf Professional Publishing: Waltham, MA, USA, 2020; pp. 1–6, ISBN 978-0-12-801898-9.
4. Khan, R., Kuru, E., Tremblay, B., Saasen, A., “Extensional Viscosity of Polymer Based Fluids as a Possible Cause of Internal Cake Formation”, *Energy Sources A*, 2007, 29, 1521–1528. DOI: [10.1080/00908310600626630](https://doi.org/10.1080/00908310600626630)
5. ANSI/API 13B-1. Recommended Practice for Field Testing Water-based Drilling Fluids, 5th ed., API Publishing Services, Washington, DC, USA, 2019.
6. Green, J., Patey, I., Wright, L., Carazza, L., Saasen, A., “The Nature of Drilling Fluid Invasion, Clean-Up, and Retention during Reservoir Formation Drilling and Completion”, SPE-185889-MS, SPE Bergen One Day Seminar, Bergen, Norway, 2017. DOI: [10.2118/185889-MS](https://doi.org/10.2118/185889-MS)
7. Nelson, P.H., “Pore-throat sizes in sandstones, tight sandstones, and shales. AAPG Bull. 2009, 93, 329–340. DOI: [10.1306/10240808059](https://doi.org/10.1306/10240808059)
8. Klungtvedt, K.R., Khalifeh, M., Saasen, A., Berglind, B., Vasshus, J.K., “Preventing Drilling Fluid Induced Reservoir Formation Damage”, SPE-202187-MS, To be published in: SPE/IADC Middle East Drilling Technology Conference and Exhibition,, Abu Dhabi, UAE, 25-27 May 2021.
9. Klungtveit, K.R., Saasen, A., Vasshus, J.K., Trodal, V.B., Manda, S.K., Berglind, B. and Khalifeh, M., “The Fundamental Principles and Standard Evaluation for Fluid Loss and Possible Extensions of Test Methodology to Assess Consequences for Formation Damage”, *Energies*, **14**(8), paper 2252, 2021. DOI: [10.3390/en14082252](https://doi.org/10.3390/en14082252)

Appendix A - Recipes

Appendix A contains the recipes for creating the different samples. Table A1 shows the components and mixing sequence for base fluid 1, Table A2 shows the components and mixing sequence for base fluid 1, and Table A3 shows which base fluid and additives were used in each sample. After all components were added to each sample, it was mixed for another 5 minutes.

Table A1-Recipe and mixing sequence of Base fluid 1.

Mixing order	Component	Amount	Mixing duration
1	Water	340g	
2	Soda Ash (Na ₂ CO ₃)	0.02g	10s
3	Caustic Soda (NaOH)	0.25g	10s
4	Xanthan Gum	1.2g	5min
5	PAC-LV	5.0g	5min
6	Magnesium Oxide (MgO)	1.0g	30s
7	Potassium chloride (KCl)	17.5g	1min
8	Additive 1		30s
9	Additive 2		30s

Table A2-Recipe and mixing sequence for Base fluid 2.

Mixing order	Component	Amount	Mixing duration
1	Water	350g	
2	Soda Ash (Na ₂ CO ₃)	0.02g	10s
3	Caustic Soda (NaOH)	0.25g	10s
4	Additive 1		5min
5	Additive 2		5min
6	Magnesium Oxide (MgO)	1.0g	30s
7	Potassium chloride (KCl)	17.5g	1min
8	Calcium Carbonate (CaCO ₃)	20.0g	30s
9	AURACOAT UF	5.0g	30s

Table A3-Base fluid and additives used in each sample.

Sample number	Base fluid:	Additive 1	Additive 2
1	1	-	-
2	1	10g Bentonite	-
3	1	10g CaCO ₃	-
4	1	10g Micronized barite	-
5	1	-	5g AURACOAT UF
6	1	10g Bentonite	5g AURACOAT UF
7	1	10g CaCO ₃	5g AURACOAT UF
8	1	10g Micronized barite	5g AURACOAT UF
9	2	2.5g Polymer A	5g PAC-LV
10	2	2.5g Polymer A	3g Polymer B
11	2	2.5g Polymer A	6g Starch
12	2	1.2g XC	5g PAC-LV
13	2	1.2g XC	5g PAC-LV
14	1	20g CaCO ₃	-
15	1	20g CaCO ₃	5g AURACOAT UF

Appendix B – Example of permeability calculations

Darcy's law was used for calculating the permeability of the discs, and rearranged to the following form:

$$K = \eta \frac{Q * \Delta L}{A * \Delta P}, \quad \text{where}$$

K is the calculated permeability [m²]

*η is the viscosity of the fluid [Pa * s]*

Q is the measured flowrate [m³/s]

ΔL is the thickness of the disc [m]


A is the areal of flow on the the disc [m²]

ΔP is the differential pressure over the disc [Pa]

Table B1 shows the chart used for permeability calculations for the disc used with Sample 13. There are many factors involved with the calculations, and because of this, some simplifications have been made. The temperature is recorded and used for calculating the viscosity. To calculate the viscosity, η , a linear interpolation was applied using data on the viscosity of air and water at different temperatures. The pressure was recorded directly from the pressure sensor and given in bar, which was converted to pascals. There is also some pressure drop in the system, which is accounted for by subtracting the flow rate multiplied by a constant factor from the measured pressure. This assumes constant pressure drop for all flow rates. The flow rate is measured directly, and converted from l/min to m³/s.

To reduce the uncertainty, 4 measurements of both pressure and flow rate was recorded, and the average was reported as the disc permeability. For air this was done by adjusting the pressure, using the regulator. For all discs the flow rate was recorded at pressures of 0.018, 0.027, 0.035 and 0.040 bar. For water this done differently. The pressure and flow rate were recorded each time the height of the water column reached a line marked on the cylinder. The distance between each line is 5 cm, which is accounted for using the formula for hydrostatic pressure. The recorded pressure in the chart, will be the pressure given on the pressure sensor + the additional hydrostatic pressure from the water column. The area of flow of the disc, is slightly less than the disc area, as the edge of the disc rests on the mounting in the cylinder.

Table B1-Permeability calculation chart used for Sample 13.

 <small>EUROPEAN MUD COMPANY</small> <small>smart fluid technology</small>			PERMEABILITY TEST		KCI-XC PAC L CC ACUF	
			Disc #:	D83	Date:	08.03.2021
			Disc grade (μ)	20	Sign:	
BEFORE						
Dry disc (g)	Air temp:	21,8		Water temp	19,7	
40,959	Instr.Press.	Flow rate	Calc.Perm	Instr.Press.	Flow rate	Calc.Perm
	0,018	4,12	2,41070503	0,257	1,84	2,86773267
	0,027	6,32	2,49193624	0,251	1,78	2,84026293
	0,035	8,22	2,50435652	0,246	1,73	2,81635217
	0,04	9,38	2,49868684	0,24	1,69	2,82005153
		Average	2,47642116		Average	2,83609983
AFTER HTHP						
Disc with cake (g)	Filtercake lift-off pressure:			Water temp		
52,58				Pressure	Flow rate	Calc.Perm
Comment:	0.5bar					#DIV/0!
	instant lift off					#DIV/0!
	flow ~ 4.8 l/min					#DIV/0!
						#DIV/0!
					Average	#DIV/0!
AFTER BREAKER OR ACID						
Wet disc (g)				Water temp	21	
				Pressure	Flow rate	Calc.Perm
Comment:				0,255	1,68	2,55456077
				0,25	1,62	2,51220877
				0,244	1,57	2,49437983
				0,239	1,52	2,46520297
					Average	2,50658809
FINAL DRYING						
Dry disc (g)	Air temp:	23,3				
40,972	Pressure	Flow rate	Calc.Perm			
	0,018	4,07	2,36789814			
	0,027	6,26	2,45690905			
	0,035	8,12	2,45923415			
	0,04	9,18	2,42018838			
		Average	2,42605743			
Retained permeability		Air	98,0 %	Water	Reverse flow	#DIV/0!
Disc mass increase		0,013			Breaker/acid	88 %

Appendix C – Research article

Starting on the next page, the article where some of these results are published is attached: Klungtveit, K.R., Saasen, A., Vasshus, J.K., Trodal, V.B., Manda, S.K., Berglind, B. and Khalifeh, M., “The Fundamental Principles and Standard Evaluation for Fluid Loss and Possible Extensions of Test Methodology to Assess Consequences for Formation Damage”, *Energies*, **14**(8), paper 2252, 2021.

Article

The Fundamental Principles and Standard Evaluation for Fluid Loss and Possible Extensions of Test Methodology to Assess Consequences for Formation Damage

Karl Ronny Klungtvedt ^{1,2,*}, Arild Saasen ² , Jan Kristian Vasshus ¹ , Vegard Bror Trodal ², Swapan Kumar Mandal ¹, Bjørn Berglind ¹ and Mahmoud Khalifeh ²

- ¹ European Mud Company AS, 4033 Stavanger, Norway; jkv@emcas.no (J.K.V.); sm@emcas.no (S.K.M.); bb@emcas.no (B.B.)
- ² Department of Energy and Petroleum Engineering, University of Stavanger, 4021 Stavanger, Norway; arild.saasen@uis.no (A.S.); vegardtrodal@gmail.com (V.B.T.); mahmoud.khalifeh@uis.no (M.K.)
- * Correspondence: krk@emcas.no



Citation: Klungtvedt, K.R.; Saasen, A.; Vasshus, J.K.; Trodal, V.B.; Mandal, S.K.; Berglind, B.; Khalifeh, M. The Fundamental Principles and Standard Evaluation for Fluid Loss and Possible Extensions of Test Methodology to Assess Consequences for Formation Damage. *Energies* **2021**, *14*, 2252. <https://doi.org/10.3390/en14082252>

Academic Editor: Ergun Kuru

Received: 17 February 2021

Accepted: 15 April 2021

Published: 16 April 2021

Publisher's Note: MDPI stays neutral with regard to jurisdictional claims in published maps and institutional affiliations.



Copyright: © 2021 by the authors. Licensee MDPI, Basel, Switzerland. This article is an open access article distributed under the terms and conditions of the Creative Commons Attribution (CC BY) license (<https://creativecommons.org/licenses/by/4.0/>).

Abstract: Industry testing procedures such as ANSI/API 13B-1 describe a method for measuring fluid loss and studying filter-cake formation against a medium of either a filter paper or a porous disc, without giving information about potential formation damage. Considering the thickness of the discs, it may also be possible to extend the method to gain an insight into aspects of formation damage. A new experimental set-up and methodology was created to evaluate changes to the porous discs after HTHP testing to generate insight into signs of formation damage, such as changes in disc mass and permeability. Such measurements were enabled by placing the disc in a cell, which allowed for reverse flow of fluid to lift off the filter-cake. Experiments were conducted with different drilling fluid compositions to evaluate the use of the new methodology. The first test series showed consistent changes in disc mass as a function of the additives applied into the fluid. The data yield insights into how the discs are sealed and to which degree solids, fibers or polymers are entering the discs. A second series of tests were set up to extend the procedure to also measure changes in the disc's permeability to air and water. The results showed that there was a positive correlation between changes in disc mass and changes in permeability. The conclusions are that the methodology may enable identifying signs of formation damage and that further studies should be conducted to optimize the method.

Keywords: fluid loss; formation damage; lost circulation; drilling fluids; filter-cake removal

1. Introduction

Different types of lost circulation materials (LCMs) are available for preventative or reactive treatment of fluid loss using procedures such as ANSI/API 13B-1 [1]. Categorization of such materials has been conducted; however, due to different application methods and different design criteria, no consistent evaluation method has been established [2]. For sealing of larger fractures, testing using slotted discs are often used and maximum sealing pressures measured. Jeennakorn et al., 2017 and 2018 [3,4] showed that varying testing conditions might give different results when testing lost circulation materials. Variations in drilling fluid compositions such as using different base fluids, density, and weighting materials impact LCM performance. Additionally, it was shown that different time-dependent degradation could occur under severe downhole conditions.

In 2018, Alshubbar et al. [5] studied the performance of LCM under conditions of an annular flow of fluid. By varying the circulation rates, they found that higher circulation rates led to higher fluid losses before a seal could be established. In addition, they identified that LCM with lower specific gravity was less prone to variations in the circulating conditions making them better preventative approach candidates.

Alsaba et al., 2014 [6] concluded that fibrous materials showed the best performance among conventional LCM in terms of sealing fractures in tapered discs and in maintaining the integrity of the formed seal within the fractures. They obtained sealing pressures up to 20.2 MPa (2925 psi) before failure when sealing a disc with a 1.0 mm fracture tip. Further, they concluded that the superior performance of the fibrous materials was considered to be due to the wide range of particle sizes and the irregularity in particle shapes and degree of deformability. In contrast, they concluded that granular materials such as CaCO₃ and graphite formed seals with relatively low integrity. In 2019, Khalifeh et al. [7] conducted high-pressure slot testing of fiber-based LCM demonstrating sealing performance where the seal did not fail even with pressures of more than 34.5 MPa (5000 psi) being applied. Further, it was shown that seals were dynamically built to withstand higher differential pressure.

Saasen et al., 2018 [8] tested lost circulation materials using a coarse gravel bed in addition to testing on slotted discs with the objective of testing materials for healing severe losses of drilling fluid to the formation. They found that addition of short fibers reduced filtration in porous formations and that use of long fibers may heal severe losses in fractured formations. Lee et al., 2020 [9] conducted parametric studies in numerical simulations to better understand thermal effects of sealing mechanisms of lost circulation materials. By studying properties such as fluid viscosity, particle size, friction coefficient, and Young's modulus they found that thermally degraded properties lead to inefficient fracture sealing.

In 1975, Enstad [10] described how dry powders might block hoppers with openings several times larger than the size of the dry powders. However, when transferring particles in a liquid or drilling fluid, different mechanisms will interact and change the particle plugging behavior. Whitfill 2008 [11] proposed a method for selecting a particle size distribution (PSD) based on the expected fracture width, where the D50 value should be equal to the fracture width to ensure the formation of an effective seal or plug. In 2015, Alsaba et al. [12] studied lost circulation materials of different shapes and their ability to seal fractures up to 2000 µm. They concluded that PSD had a significant effect on the seal integrities, and in particular the D90 value. It was found that a D90 value, which was equal or slightly larger than the fracture width, was required to initiate a strong seal. When combined with finer particles, the permeability of the seal would be lower, and the fluid loss reduced. A study of sealing pressure prediction [13] also found that in after the fracture width and fluid density, the D90 value was the most significant influence of sealing pressure.

The observation of particle size degradation of CaCO₃ and graphite, primarily due to the influence of shear, was also observed by Hoxha et al., 2016 [14]. In their studies the D50 values of medium grade CaCO₃ decreased by 25–40% after 30 min of shearing. Further, it was found that various methods for measuring the PSD yielded different results. As an example, the change in D50 value of regular grade graphite was recorded to be reduced between 20% to circa 70%.

In 1999, Pitoni et al. [15] studied how changes in solids composition of reservoir drilling fluids impacted forming of filter-cakes and return permeabilities. They found that filter-cake became softer and thickness increased with increasing solids content in the fluid. However, they observed that the higher the clay content, the thinner and harder the filter-cake. Additionally, the fluids with higher clay contents gave a lower return permeability. They also concluded that the size of the bridging particles effectively could be increased for high permeability or poorly consolidated formations, by adding coarse bridging particles and running the system in a "sacrificial" manner.

When conducting core flood studies to assist in designing of drilling and completion fluids in 2017, Green et al. [16] found that the lowest permeability alterations did not correlate with the lowest drilling fluid filtrate loss volumes. They concluded that the major formation damage is more likely to be caused by the drilling fluid filter cake's ability to stick to the formation and whether it can be removed during production.

Czuprat et al., 2019 [17] conducted experiments with long-term (14 days) static aging of drilling fluids and testing of fluid properties including filtration behavior and formation damage tests on sandstone samples and reservoir rock. They concluded that lower solids content in the drilling fluid would result in a slower build-up of the filter-cake, thus allowing for a higher amount of fluid filtrate invasion to occur. Additionally, they concluded that the long test period might be impractical for a service company to conduct tests before selecting a drilling fluid.

When drilling a reservoir formation with a water-based drilling fluid, polymers are used to provide viscosity and to control filtration losses. Khan et al. [18] showed that polymers such as xanthan gum, long-chain poly anionic cellulose (PAC) and starch may help in reducing fluid losses to the formation. If the pore-throats are exceeding, e.g., 20 μm and differential pressures exceeding 3.45 MPa (500 psi), such polymer additives may have little effect in preventing solids from entering the formation. PAC with shorter chains and lower viscosity (PAC LV) impact are used to reduce fluid losses through their bonding to solids in the drilling fluid and to pore-throats in the formation.

Cobianco et al., 2001 [19] developed a drill-in fluid for low permeability reservoirs using a fluid consisting of biopolymers, highly crosslinked starch and microfibrinous cellulose. The used Portland limestone cores with permeability of ca. 20–100 mD for static filtration tests at differential pressures ranging from 1 to 3 MPa (145–435 psi) at 80 °C and backflowed with a 3% KCl brine to measure permeability to brine. They found that when the drilling fluid including cuttings, the return permeability was slightly lower than the formulation without the cuttings. SEM micrographs indicated that cuttings invasion was limited to the first 100 μm .

Nelson 2009 [20] conducted a study on pore-throat sizes in siliciclastic rocks and found that they form a continuum from the submillimeter to the nanometer scale. He found that reservoir sandstones generally have pore sizes greater than 20 μm and pore-throat sizes greater than 2 μm . The data reported by Nelson are hence consistent with also using discs with a median pore-throat size of 20 μm to represent a sandstone formation.

Reservoir formation damage may take place through different mechanisms [21]. It is a generic term that refers to impairment of the permeability of petroleum-bearing formations by various adverse processes. The impairment may take the form of a mechanical mechanism, such as, e.g., fines migration, solids invasion or phase trapping, or in the form of biological mechanisms or chemical mechanisms.

The literature shows that test procedures (e.g., types of fluids, applied pressure and temperature, type of flooded medium, type and geometry of LCM, etc.) create inconsistency in results obtained by different researchers. Some research study changes in formation damage by measuring changes in permeability to a fluid using rock cores. These cores are of a different nature than the discs used for the day-to-day testing of fluid loss, as per ANSI/API13B-1, thereby making such testing less accessible for a researcher or a fluid engineer.

Therefore, in this article, experiments were set up to understand the data set that is typically collected when conducting HTHP test according to ANSI/API13B-1. Thereafter, new testing methods are investigated to identify if new information about fluid loss and formation damage could be collected by extending the test procedures and using the same permeable discs. The overall objective is to use such methods for further product development and evaluation or optimization of drilling fluids. If cost-effective test methods can be established, it will facilitate more effective research and more consistent comparison of various drilling fluid compositions. The objective of the research was to identify a cost-effective method for testing drilling fluids and drilling fluid additives and to verify if this method could be used to provide reliable information about formation damage or indication of formation damage. The introduction of a moisture analyzer to precisely measure the mass change of the discs may be such a cost-effective method for identifying formation damage.

2. Analytical Approach

An experimental setup was therefore built with the following main objectives and functionalities:

- Enabling reverse flow of a fluid through the discs, after the HTHP tests, to understand filter-cake lift-off pressures.
- Enabling measurement of disc mass before and after the HTHP test and filter-cake removal to obtain indications of polymer or solids invasion into the discs.
- Enabling disc permeability estimation before and after the HTHP test and filter-cake removal to obtain indications of changes in disc permeability.
- Studying fluid loss profiles and filter-cake building.
- Establishing a practical routine for application of breaker fluid or acid to remove filter-cake.
- Understanding how various fluid degradation methods may impact the fluid loss and reservoir formation damage.

In order to investigate these potential changes in methodology, the two different base fluids shown in Appendix A, Tables A1 and A5 with KCl, xanthan gum and PAC were used. The effect of incorporation of different solids particles in the form of bentonite, CaCO₃, micronized barite and three types of cellulose-based fibers was investigated. The objective of using different base fluids and different fibers was to verify if the methodology could be valid for different types of fluid compositions. As the verification on the methodology was the primary objective of the research, the actual product names are not used in the descriptions. Experiments were set up with discs of mean pore-throats of 20 µm, 120 µm and 250 µm to reflect different permeability formations.

2.1. Key Factors in Fluid Loss Measurement Using Water-Based Drilling Fluids

Field engineers evaluate the properties of drilling fluid during operations to understand the requirement for potential treatment of the fluid to obtain certain desired parameters. One of these tests will normally be an HTHP test to understand filter-cake properties and the drilling fluid's ability to create a temporary seal against permeable formation.

2.1.1. Equipment for Testing According to ANSI/API 13B-1

In addition to conventional laboratory equipment for mixing (e.g., hot-rolling drilling fluids, pH and rheology measurements), the primary equipment required is an HTHP cell, which allows for testing on filter paper and permeable discs. In the experiments that were conducted, the following equipment was used:

- Hamilton Beach Mixer, Virginia, USA;
- Ohaus Pioneer Precision PX3202, New Jersey, USA;
- Ofite Filter Press HTHP 175 mL, Double Capped, Texas, USA;
- Ofite Viscometer model 900, Texas, USA;
- Ofite roller-oven #172-00-1-C, Texas, USA;
- Apera pH90, pH meter, Wuppertal, Germany.

2.1.2. Test Procedure and Data Collection in Accordance with ANSI/API 13B-1

For the full procedure, please refer to the ANSI/API 13B-1 for water-based drilling fluids or ANSI/API 13B-2 for oil-based drilling fluids [22]. The information contained herein contains only the main elements. The filtration tests are conducted at high temperature and high pressure under static conditions using a pressurized gas source to create a differential pressure across the test medium. The test medium used is either a filter paper, typically with a median pore-throat of 2.5 µm or permeable ceramic discs with means pore throats ranging from 10 to 250 µm. After the differential pressure has been applied and the temperature in the cell has reached the desired level, the cylinder outlet valve is opened to enable the differential pressure to drive the fluid towards the medium. The fluid filtrate

is thereafter collected and measured over a 30-min period. For comparison with other tests, one needs to account for differences in filter area. The data collected according to the procedure is:

- Measure the filter-cake thickness, at its center, to the nearest millimeter (or 1/32 in).
- Observe indications of settling of solids on the filter-cake, such as an abnormally thick cake or coarse texture, and record comments.
- The filtrate volume V_f should be measured and normalized with regards to filter area.

2.2. Extending the HTHP Filtration Tests to Study Signs of Formation Damage

The objective is to collect information related to formation damage and other operational parameters and to identify if the methodology can yield meaningful information about potential formation damage.

2.2.1. Equipment Overview

The experimental set-up was centered around a cell with regulated supply of pressured air to drive a fluid or air through the ceramic discs. The experiments were not planned for filter paper, as the filter paper is not designed for higher pressures than 3.45 MPa (500 psi). By reversing the discs into the cell, fluid can be pumped through the disc at low pressures to study the lift-off pressure of filter-cakes, as shown in Figure 1. Further, by measuring both the supply pressure and flowrate, estimates of disc permeability could be conducted. Extending the procedure further, a moisture analyzer was used to measure the mass of the disc in a standardized dry condition before the HTHP test and after the test including reverse flow and any breaker application. The following equipment was used for the experimental set-up in addition to the standard equipment used for the HTHP test according to ANSI/API 13B-1:

- Ohaus MB120 Moisture Analyzer;
- Custom built transparent acrylic cell with stand for enabling of reverse flow of fluid through the ceramic discs;
- Festo pressure regulator LRP-1/4-2.5 and LRP-1/4-0.25;
- Festo Pressure Sensor SPAN-P025R and SPAN-P10R;
- Festo Flowmeter SFAH-10U;
- Nitrogen source and manifold for pressure up to 9.3 MPa (1350 psi), Ofite #171-24;
- Vacuum machine, DVP EC.20-1.

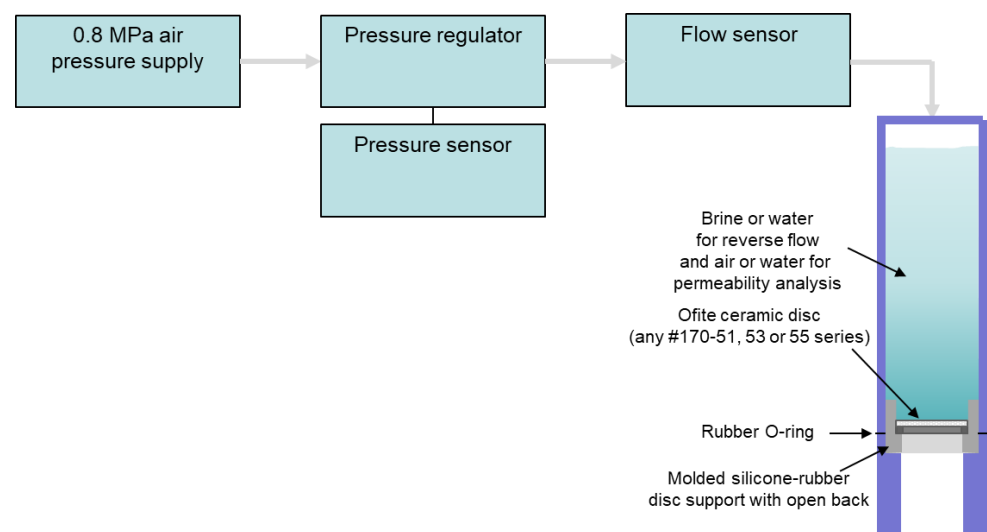


Figure 1. Infographic of the system developed for this study.

2.2.2. Procedures Applied for Testing Using Experimental Set-Up

The main elements of the new procedure are the measurement of disc mass and permeability to water and air before and after the HTHP test. For the full procedure and calculations, please refer to Appendix B. Testing of permeability was restricted to discs with mean pore-throat size of 20 μm as it was difficult to establish precise readings of pressure and flow rate with flow of air or water through the higher permeability discs. A permeability analysis of other disc grades may be practical with a higher viscosity fluid. Otherwise, the procedure was the same for all ceramic disc grades.

3. Experimental Data

3.1. Identifying Signs of Polymer, Solids or Fiber Invasion into Permeable Formations Using a Moisture Analyzer to Measure Changes in Disc Mass

In total, 11 different samples were tested according to the procedure described in Appendix B, including 16 h of hot-rolling at 90 $^{\circ}\text{C}$, six of which were tested on ceramic discs with a specified median pore-throat size of 120 μm (Ofite #170-53-4) and five of which were tested on 250 μm discs (Ofite #170-53-6). All tests were conducted at 6.9 MPa (1000 psi) differential pressure and 90 $^{\circ}\text{C}$. An overview of the tests is shown in Table 1. Fiber A and Fiber B were selected from two different manufacturers of cellulose-based lost circulation materials, based on relatively similar specified particle size distributions.

Table 1. Test overview for high-permeability discs.

Test Number	Description of Test
1	Base fluid (with bentonite and CaCO_3), normal mixing, 120 μm disc
2	Base fluid, high-shear mixing, 120 μm disc
3	Base fluid, high-shear mixing, 250 μm disc
4	Base fluid plus FIBER A, normal mixing, 120 μm disc
5	Base fluid plus FIBER A, high-shear mixing, 120 μm disc
6	Base fluid plus FIBER A, normal mixing, 250 μm disc
7	Base fluid plus FIBER A, high-shear mixing, 250 μm disc
8	Base fluid plus FIBER B, normal mixing, 120 μm disc
9	Base fluid plus FIBER B, high-shear mixing, 120 μm disc
10	Base fluid plus FIBER B, normal mixing, 250 μm disc
11	Base fluid plus FIBER B, high-shear mixing, 250 μm disc

Five of the tests were conducted after a 30-min high-shear mixing procedure to identify any particle degradation. The same degradation test was conducted separately for some of the wet-sieving tests referenced in Figure 2. The degradation tests indicated that CaCO_3 degraded partially during the high-shear mixing procedure. Initially, the wet sieving showed 15.7% and 15.8% of particles being larger than 90 μm , equivalent to a concentration of 13.4–13.5 kg/m^3 in the respective fluid samples. After the high-shear mixing, the concentrations of particles larger than 90 μm was reduced to 9.7% and 9.2%, respectively, implying that circa 40% of the particles above 90 μm had been degraded, and that the resulting concentrations in the fluid samples would be 8.3 kg/m^3 and 7.9 kg/m^3 . In contrast, the high-shear mixing of FIBER A did not show signs of degrading, and the concentration was kept stable around 10.6 kg/m^3 . One test, which included bentonite, showed an increase in concentrations of FIBER A above 90 μm after high-shear mixing. Since the high-shear mixing of FIBER A without bentonite did not show the same effect, it was considered that a potential cause of the apparent increase in the concentration of larger particles may be bentonite particles piggybacking on the coarser FIBER A particles

to increase the measured concentration of such particles. Tables A2 and A3 in Appendix A gives more detailed information about dry sieving and wet sieving results.

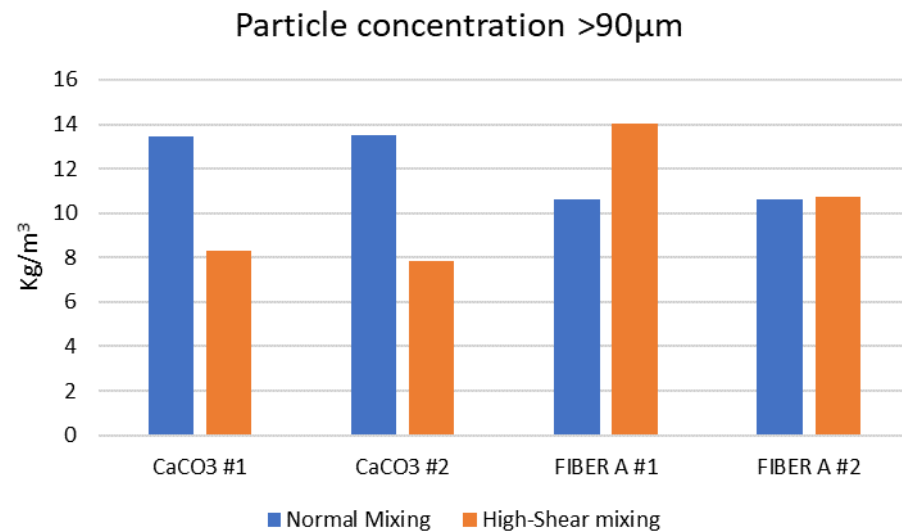


Figure 2. Changes in particle concentration in fluid due to high-shear degradation.

Figure 3 shows the HTHP tests on the 120 μ m discs on the left, with each of the three mixtures of (i) the base fluid being KCl-Polymer drilling fluid with CaCO₃, (ii) the base fluid plus FIBER A, and (iii) the base fluid plus FIBER B. The tests were conducted with and without high-shear degradation. The fluid loss tests showed that the base fluid produced a fluid loss of 31 mL before degradation and that the fluid loss increased to 42 mL after degradation. The fluid with FIBER A showed a fluid loss of 31 mL before degradation, but unlike the base fluid, the sealing efficiency increased after the high-shear degradation and gave a fluid loss of 25 mL. The fluid with FIBER B also showed an improvement after the degradation test, where the fluid loss was 45 mL without degradation and just over 31 mL after degradation.

The fluid loss profiles were generally consistent throughout the testing on the 120 μ m discs. After the initial spurt-loss, the loss-rates were gradually falling during the test and appeared to approach a linear curve with a fluid loss rate of around 0.2 mL/min after 20 min. The development of the fluid loss may indicate that the filter-cake had substantially been formed within the first 15 s, but that further thickness was built over time and that a more stable permeability achieved after 10–20 min.

The testing on 250 μ m discs, shown in the right half of Figure 3, was planned to be identical to the testing on the 120 μ m disc, however, the base fluid with CaCO₃ recorded a total loss during the first few seconds of the test, so no further tests were conducted with the base fluid alone. The testing of the two fiber-based products FIBER A and FIBER B showed considerably improved results relative to the testing on the 120 μ m ceramic. Contrary to expectations, the fluid losses recorded on the 250 μ m discs were significantly smaller than on the 120 μ m disc, and the fluid loss rates were showing a different profile. Again, the tests showed lower fluid losses after the high-shear degradation tests. The main difference, however, was the observation of more erratic fluid losses during the 30-min test. It was several times observed that the fluid loss appeared to stop, and then restarted again at more irregular intervals.

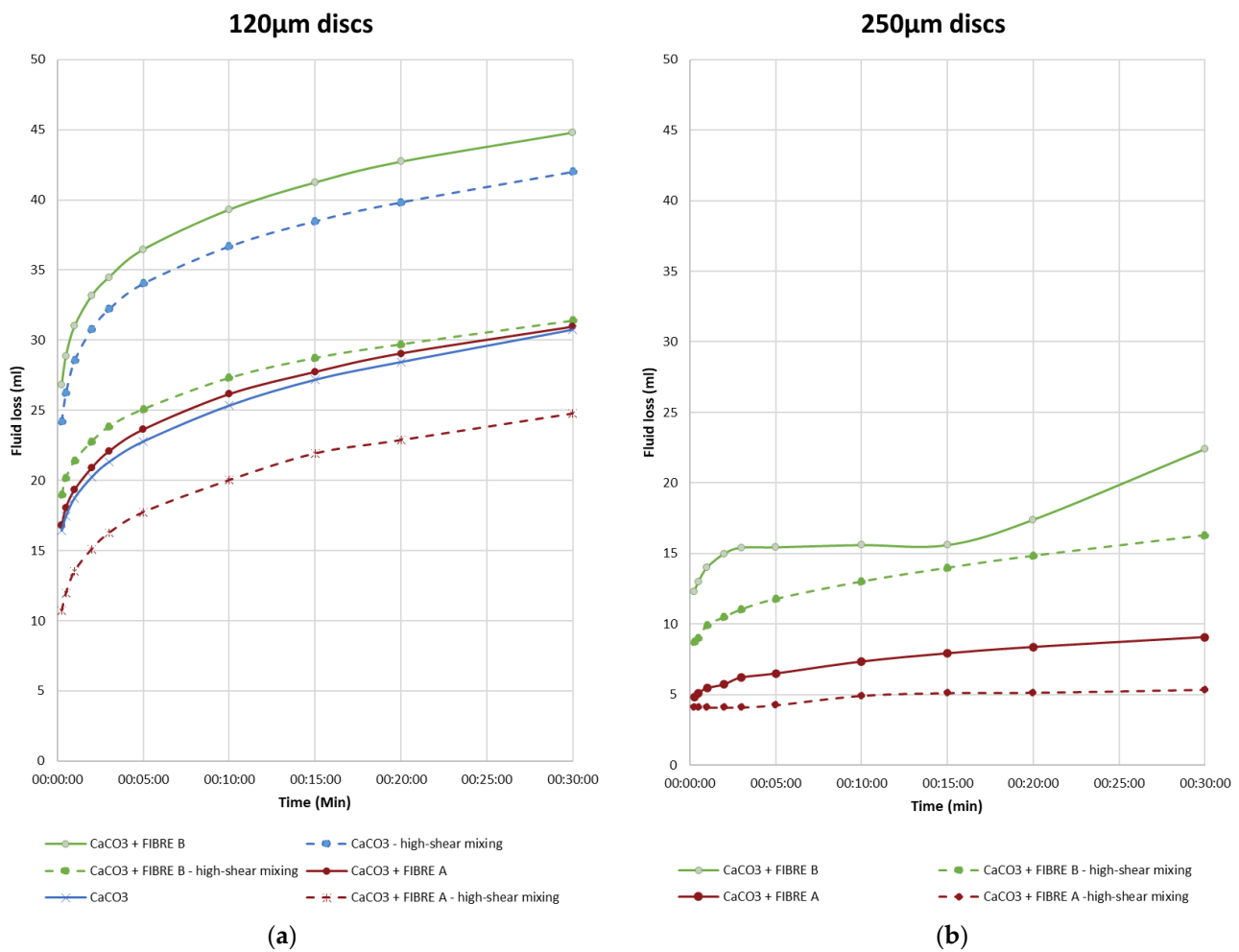


Figure 3. Fluid loss on high-permeability discs, (a) 120 μm discs and (b) 250 μm discs.

By comparing the filter-cakes from the different tests, it was clear that the building of the filter-cakes followed a different mechanism on the coarser discs. The filter-cakes formed on the 120 μm discs were of a uniform nature and thicker than the more irregular filter-cakes on the 250 μm discs, as seen in Figure 4. The impression was that the combined particles of the CaCO₃ and the fibers created a layered mat on the surface of the 120 μm disc, whereas the single or collections of particles were plugging larger pores on the 250 μm discs.

When conducting the low-pressure reverse flow of brine through the discs (<7 psi or <0.05 MPa), the filter-cakes were easily removed from the 120 μm discs as the filter-cakes came off either whole or in large pieces. Little visual trace of the filter-cakes was left on the disc other than along the circumference, which was held back by the silicone mold, which held the disc inside the acrylic cell, see Figure 5 as an example.

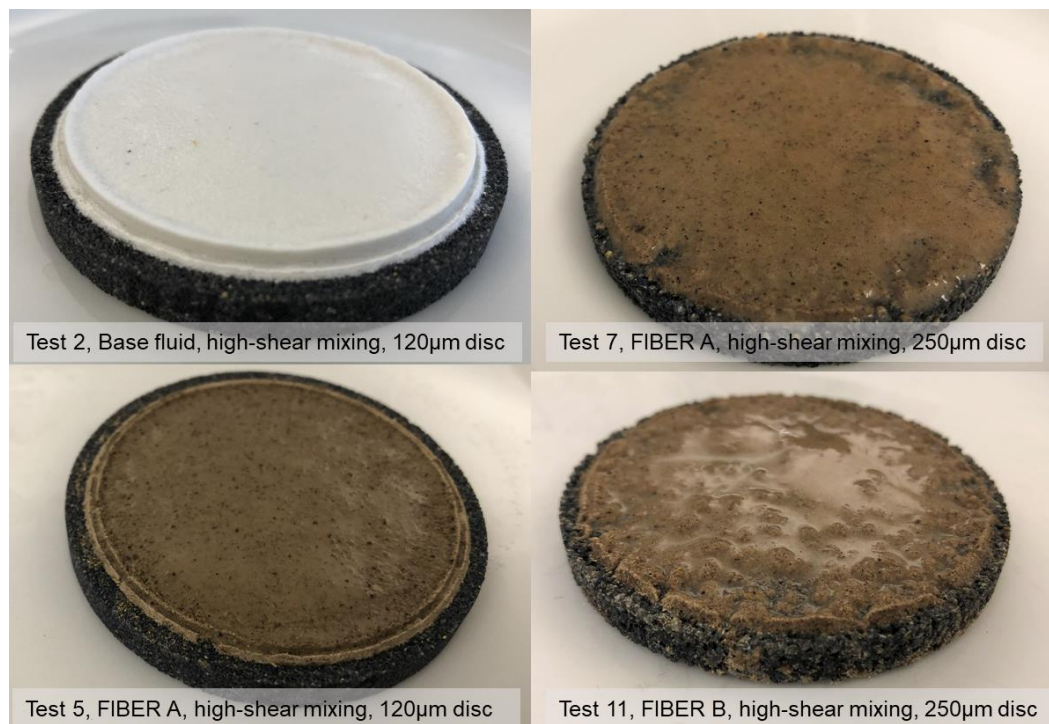


Figure 4. Filter-cakes after the 6.9 MPa (1000 psi) HTHP fluid loss test.

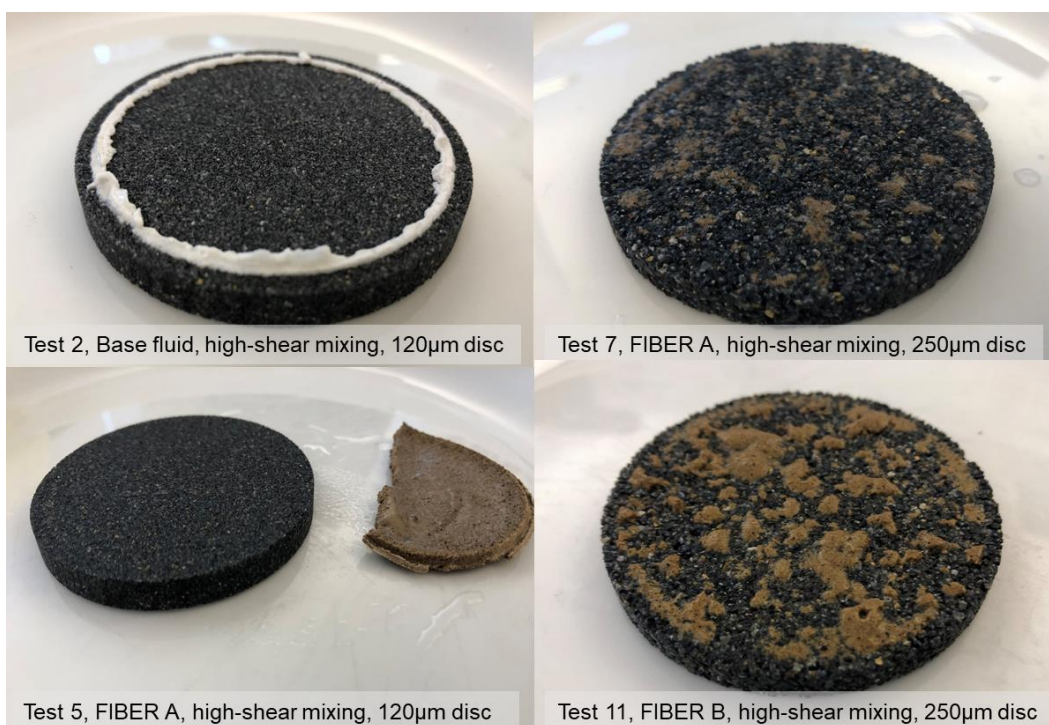


Figure 5. Discs after reverse flow with brine at 0.05 MPa pressure.

On the 250 μm discs, the filter-cakes were noticeably more separated as they were washed off the discs. This may be due to the filter-cake being thinner than for the 120 μm discs. Visual inspection showed minor particles protruding from the surface of the discs, giving further substance to the impression of particles partly penetrating and plugging the pore-throats of the discs.

Following the reverse flow, the discs were placed in a liquid oxidizing breaker and kept at a temperature of 90–100 °C for four hours. The discs were thereafter flowed with water to remove any loose residue and dried in the moisture analyzer. The discs were visually inspected for traces of residue and the final disc masses compared with the original disc masses to identify any invasion of polymer, solids or fiber. Figure 6 shows the discs from testing of FIBER A after removal of filter-cakes. By visual inspection no particle or filter-cake residue could be identified. In contrast, some residue could be seen into the pore-throats of the 250 µm discs in Figure 7, after testing of FIBER B, thereby the indicating particle-plugging inside the disc.

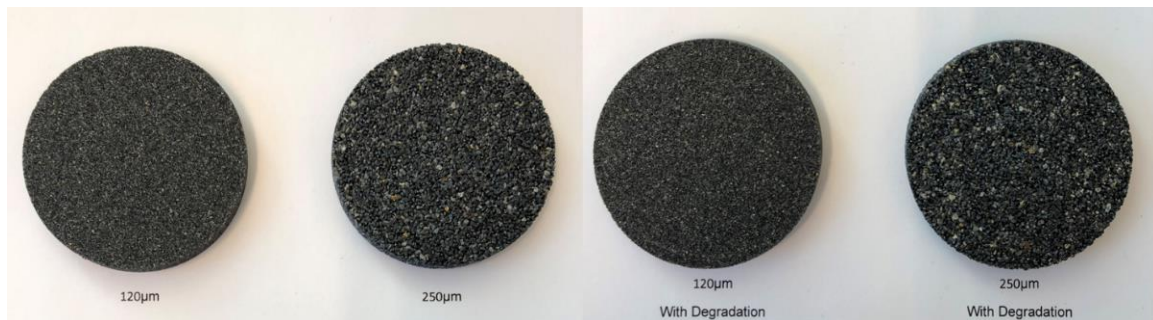


Figure 6. Discs for testing of FIBER A after breaker application.

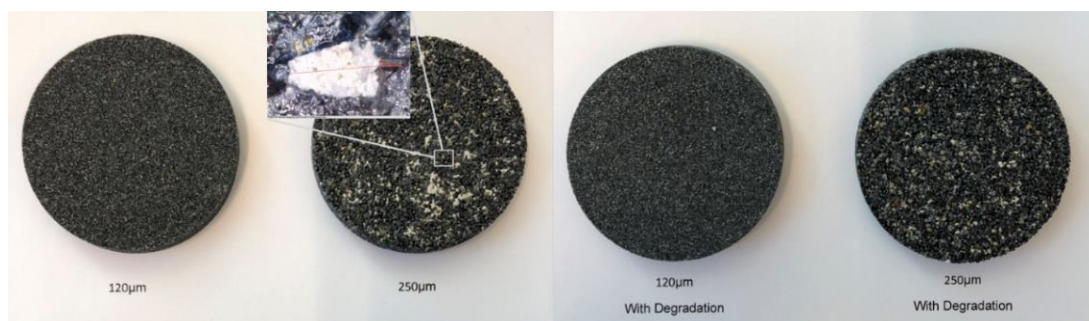


Figure 7. Discs for testing of FIBER B after breaker application.

By placing both the fluid loss measurements and disc mass gain data into one chart, some interesting observations can be made, see Figure 8.

Tests 1 and 2 with the base fluid including CaCO_3 show that nearly all of the filter-cake and potential invasion of polymers and solids into the discs have been removed by the reverse flow and breaker application. In contrast, test number 3 recorded a total loss of fluid and no pressure control. This corresponded with a more significant increase in disc mass, which may be due to residue of polymers and solids. This clearly indicates that formation damage may occur when the particles are of insufficient size to create a low-permeability filter-cake.

The four tests conducted with FIBER A show an inverse relationship between increase in disc mass and fluid loss. After visual inspection of the filter-cakes, it looked like the filter-cakes on the 250 µm showed more of a particle-plugging nature, whereas the filter-cakes on the 120 µm discs to a greater extent were created uniformly and externally to the disc. The measurements of increase in disc mass were consistent with this theory, as low increases in disc mass were recorded on the 120 µm discs, and more significant increases in disc mass was recorded on the 250 µm discs, where particle plugging, or deep sealing was suspected.

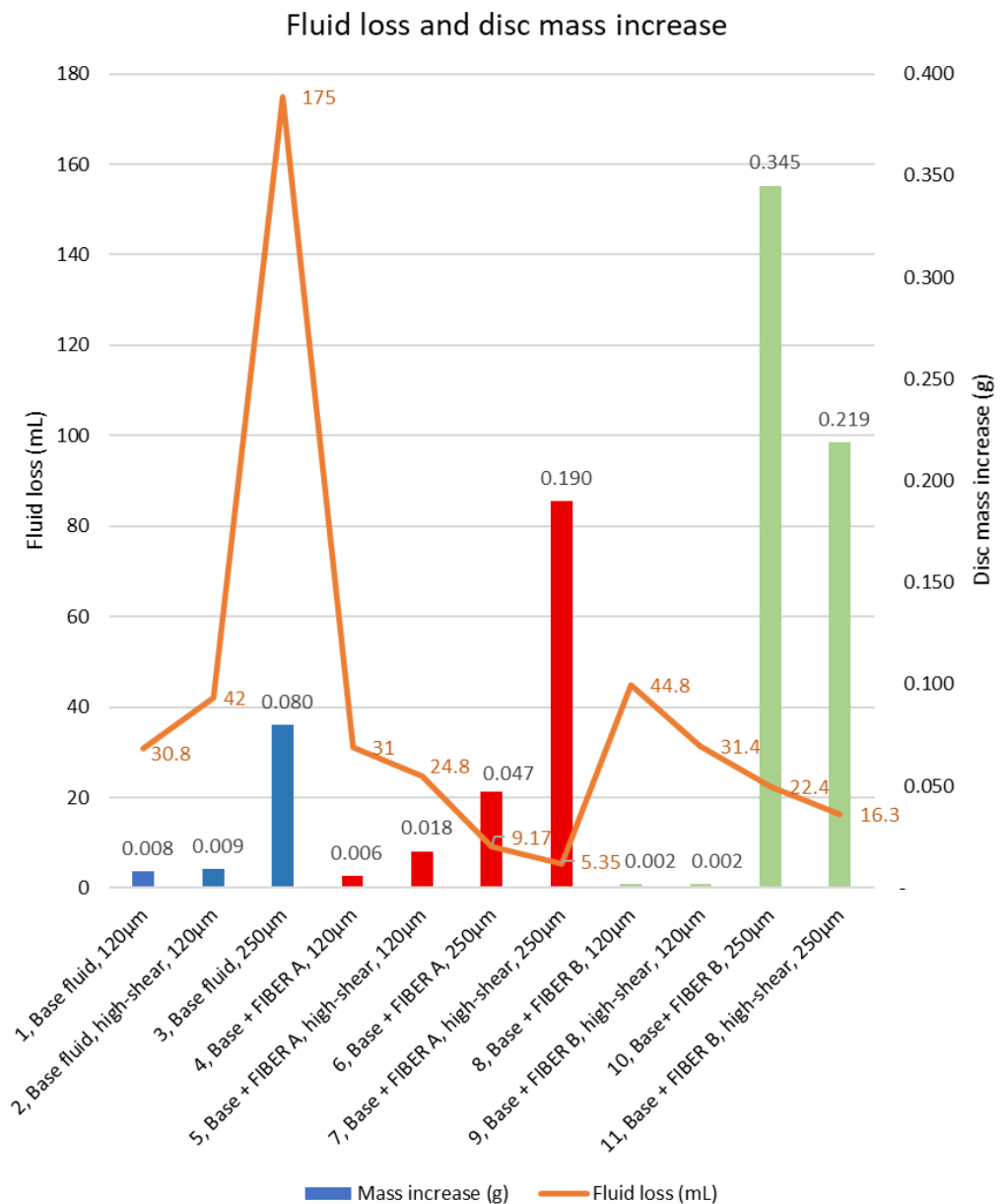


Figure 8. Fluid loss and disc mass increase.

The tests with FIBER B were consistent with the observations from the testing of FIBER A. Disc mass increases were negligible on the finer discs, whereas the mass increases of the coarser discs were the largest in the test. The full data for disc mass measurements can be found in Table A4 in Appendix A.

Dry-sieving tests indicated that both FIBER A and FIBER B had a weight concentration of 13–14% with particles larger than 180 µm, whereas only 1% of the CaCO₃ was larger than 180 µm. As such a lower sealing ability of the 250 µm discs without the presence of any of the fiber products could be expected. The sealing of the 120 µm discs was shown to be falling as the percentage of CaCO₃ particles was reduced after degradation in test number 2, relative to test number 1, as also shown in Figure 2. A 90 µm particle size represents 75% of the specified median pore-throat size of the 120 µm discs. This may be an indication that particles above 75% of the median pore-throat size of the disc may be required to form an effective filter-cake.

3.2. Extending the Testing Regime to Include Estimation of Disc Permeability Changes

A new set of tests was conducted to study potential changes in the permeability of ceramic discs with specified mean pore-throat size of 20 μm (Ofite #170–53-3). The tests were conducted using the full test-procedure specified in Appendix B. Four tests were conducted with a KCl-Polymer fluid with combinations of Bentonite and FIBER UF as sealing-materials, refer to Appendix A, Table A5 for the full recipe. Due to finer discs being used than in the tests referred to in Section 3.1, a finer grade fiber was selected. FIBER UF was provided by the vendor with a specified D90 of 75 μm and a D100 of 90 μm . The rheology of the various fluid compositions was measured before and after hot-rolling. The measurements showed slight increases in shear stress for a given shear rate as more particles were added to the fluid, as shown in Figure A1, Appendix A.

The disc grade was chosen such that it would be practical to test water-permeability and air-permeability, in addition to the changes in disc mass as described in Section 3.1. Discs with median pore-throat size larger than 20 μm were found to be more difficult to test, as the flowrates of fluid would be very high relative to the low pressures applied. Table 2 show the main data from tests 12–15. As an initial experiment, it was chosen to use water to test permeability even though this would not represent a reservoir fluid. The objective was only to ascertain if the method had practical value, rather than to be an exact replication of a reservoir drilling situation in presence of hydrocarbons.

Table 2. Fluid loss and formation damage data for tests 12–15.

Test	Fluid Loss	Disc Mass Change	Water Permeability Retention	Air Permeability Retention
12, Base fluid 2	Total loss	From 42.031 to 42.279 g = +0.248 g	From 3.338 to 0.997 D = 30%	From 2.327 to 0.822 D = 35%
13, Base fluid 2 + 14.3 kg/m ³ (5 ppb) FIBER UF	24.2 mL	From 41.394 to 41.419 g = +0.025 g	From 4.056 to 2.253 D = 56%	From 2.824 to 2.378 D = 89%
14 Base fluid 2 + 28.5 kg/m ³ (10 ppb) Bentonite	32.2 mL	From 40.776 to 40.795 g = +0.029 g	From 5.633 to 3.166 D = 56%	From 2.823 to 2.686 = 95%
15, Base fluid 2 + 28.5 kg/m ³ (10 ppb) Bentonite and 14.3 kg/m ³ (5 ppb) FIBER UF	19.8 mL	From 40.990 to 40.986 g = −0.004 g	From 5.329 to 3.459 D = 65%	From 3.479 to 3.037 D = 87%

The fluid loss data showed that the Base Fluid 2 (test 12) could not withstand the 6.9 MPa (1000 psi) pressure and build a filter-cake. The HTHP fluid loss test was therefore aborted after around 2–3 s. The reverse-flow of brine through the disc at 0.075 MPa (11 psi) showed very little fluid flow. The disc mass measurement showed that the test with the Base Fluid 2 created a significant increase in the disc mass of 248 mg. Due to the fluid not containing either solids or fiber, the disc mass increase was likely reflecting polymer damage to the formation. The measurements of permeability to water indicated that only 30% of initial permeability had been retained during the test. A thin layer of residue was visible on the surface of the disc where the filter-cake should have been formed.

Test 13 showed that the addition 14.3 kg/m³ (5 ppb) of FIBER UF could seal the disc without the presence of solids and produced a fluid loss of 24.2 mL. The reverse-flow of brine through the disc at 0.075 MPa (11 psi) showed very moderate fluid flow, but the filter-cake did not lift off directly. After application of breaker, the filter-cake was dissolved and the measurement of permeability to water showed that 56% of original permeability had been retained. The disc mass measurement showed a low increase of mass of 25 mg. Only a slight change in color on the surface showed that there had been a filter-cake on the disc prior to the application of the breaker fluid.

By adding 28.5 kg/m³ (10 ppb) of bentonite instead of the fiber, test 14 was completed with a fluid loss of 32.2 mL. Reverser flow of brine lifted off the filter-cake and fluid flow appeared relatively similar to test 13. After application of the breaker, the filter-cake was dissolved and the measurement of permeability to water showed that 56% of the original permeability had been retained. The disc mass measurement showed a low increase of

mass of 29 mg. Some light gray residue was visible on the surface of the disc after reverse flow and breaker fluid application.

The lowest fluid loss was recorded when both 14.3 kg/m^3 (5 ppb) of FIBER UF and 28.5 kg/m^3 (10 ppb) of bentonite was added to the base fluid. For this test, the fluid loss was reduced to 19.8 mL. There was no visible residue on the disc surface and the mass measurement indicated a very minor fall in disc mass of 4 mg. The measurement of permeability to water showed retention of 65%.

The information on changes in disc mass, permeability to water and air were gathered in attempt to find practical method for studying indicators of any formation damage caused by the drilling fluid in a real-life application. A differential pressure of 6.9 MPa (1000 psi) was considered to be adequately reflecting what might be experienced in certain drilling situations. Similarly, it was of interest to see if a relatively low reverse pressure of 0.075 MPa (11 psi) could start the process of filter-cake removal before any chemical cleaning of the reservoir was applied.

It was shown that the addition of either FIBER UF or bentonite reduced the invasion of drilling fluid into the formation and also that less damage appeared to have been made to the formation permeability. Further, the combination of FIBER UF and bentonite showed even lower fluid loss and the visual inspection and the mass measurement indicated that no or little damage to the formation had been caused. In contrast, the estimation of permeability to water showed that some change in permeability might have occurred. In this context one should consider the polarity of water and its potential interaction with bentonite and the cellulose based FIBER UF.

When studying the results of the tests it should be considered that only the first 6.35 mm ($1/4''$) or of the formation has been studied. The content of the fluid filtrate has not been studied, and hence it may be difficult to provide clear evidence for which further damage could have been caused to formation further away from the wellbore. During tests 13–15, the applied pressure of 6.9 MPa (1000 psi) was successfully held, and a moderate amount of fluid filtrate was collected. This may be an indication that such fluid compositions would be quite effective in preventing fluid loss to the formation. Test 12 showed that polymers alone could not seal the disc under the applied differential pressure nor prevented polymers from migrating into the disc. Figure 9 shows the discs after breaker application and drying.



Figure 9. Discs from tests 12–15 after breaker application and drying.

4. Observations and Lessons Learned from the Experimental Procedure

Measurement of disc mass using the moisture analyzer, weighing the fluid filtrate continuously during the HTHP process and calculation of fluid filtrate were practical exercises that yielded consistent results without complications.

The process of reverse flow using brine and water for lifting of filter-cake functioned very well within certain limitations. For tests where the applied differential pressure during the HTHP test was 6.9 MPa (1000 psi), certain fluid combinations showed little or no reverse flow with applied reverse pressure of 0.069 MPa (10 psi) and a brine temperature

of 60 °C. It was experimented with applying higher reverse pressures and higher brine temperatures whilst developing the method that was applied. Higher temperatures were avoided to avoid deforming of the acrylic cylinder, and higher pressures were avoided as some discs fractured if the reverse pressure exceeded 0.1 MPa (15 psi).

Calculating the average permeability to dry air functioned very well and yielded quite consistent and repeatable results on dry discs prior to any HTHP testing. The primary ambition was to identify changes to the calculated permeability of each individual disc. One observation was that the permeability of discs coming from different batches varied considerably, whereas discs coming from the same batch appeared to be more similar. The method has a weakness when used after an HTHP test as it is based on the disc being predried before flowing of air. Using this method, the effects of drying may impact discs with the presence of, e.g., polymers, solids, and fibers and their ability to obstruct flow of air differently. These data may therefore be imprecise relative to flow of fluids in a reservoir formation.

Adapting the permeability estimation to a fluid such as water appeared to be more complex. The primary observation was that the calculated permeability of an individual disc could vary, even when correcting for changes in viscosity due to temperature changes. The process that enabled a stabilization of the readings included to place the disc in fluid in vacuum to remove any air-bubbles from the disc and fluid before the test. This yielded considerably more consistent results, particularly on low-permeability discs. A cause of the uncertainty of measurement was thought to be capillary forces at the air–water interface, and the improvement obtained by placing the disc and fluid in vacuum strengthened this idea.

Additionally, it should be considered that the thickness of the discs (ΔL) is low relatively to the depth of a typical core sample for a return permeability test. The testing of the discs can therefore be considered to reflect the skin damage of a formation.

5. Conclusions

The inclusion of additional procedures to those described in ANSI/API 13B-1 yielded information relevant to obtaining a better understanding of fluid loss and giving an insight into how various drilling fluid compositions seal permeable formations and how they may impact future reservoir permeability. The main conclusions are as follows:

- By extending the testing procedure with (i) a moisture analyzer and (ii) reverse flow equipment and a procedure for reverse flow and breaker fluid application it was possible to measure the increases in disc mass accurately.
- Reverse flow of fluid through the disc with filter-cake enables studying the removal of filter-cake by back pressure.
- Application of an oxidizing breaker did in certain cases allow the test discs to return to almost its original state, with mass changes so low that they may be considered to be within the tolerances of the tests.
- As the discs median pore-throat size was varied relative to the particle size of the fibers and CaCO_3 , for tests 1–11, it appeared that different mechanisms for sealing the disc and creating a filter-cake was obtained. Hereunder, when the solids or fibers were equal or marginally smaller than the pore-throat openings, fluid loss was reduced, and the sealing appeared to partial plugging of the pore-throats. In contrast, when a significant portion of the particles was larger than the mean pore-throat size, a thicker and more uniform filter-cake was building on the disc. Without the presence of fibers or when the solids were smaller than the pore-throats, no low-permeability filter-cake was formed, and disc mass increases were significant.
- In the tests on the 120–250 μm discs where either of the fiber products was present, there was an inverse relationship between fluid loss and disc mass increases. In the tests on the 20 μm discs, the fibers appeared to be larger than the pore-throats, and there was a positive relationship between lower fluid loss and lower disc mass increase.

- Testing of disc mass change and change of permeability to water and air suggested that ranking 20 μm discs in terms of lowest increase in mass and lowest calculated change to water-permeability would yield consistent results in terms of indicating formation damage. Since the other disc grades are built up in the same way as the 20 μm discs, it may be possible to obtain equivalent results with discs of other grades.
- The findings on using the new testing methodologies are indicating that valuable information concerning reservoir formation damage may be observed and estimated using a relatively simple set-up and test procedure. To further investigate this potential, it is recommended to conduct further experiments. One of the natural extensions of the methodology is to investigate using a non-polar hydrocarbon-based fluid for testing of permeability and for presoaking discs before the fluid loss test.

Author Contributions: Conceptualization, K.R.K.; methodology, K.R.K. and J.K.V.; formal analysis, K.R.K., B.B. and V.B.T.; writing—original draft preparation, K.R.K.; writing—review and editing, K.R.K., A.S., M.K. and S.K.M.; supervision, S.K.M. All authors have read and agreed to the published version of the manuscript.

Funding: This research was funded by The Research Council of Norway, grant number 320646, Innovation Norway, grant number 2020/527515 together with European Mud Company AS.

Institutional Review Board Statement: Not applicable.

Informed Consent Statement: Not applicable.

Data Availability Statement: Data availability on request due to intellectual property rights of EMC.

Conflicts of Interest: The authors confirm that this article content has no conflict of interest.

Appendix A

Appendix A contains recipes and data from the tests.

Table A1. Recipe and mixing sequence of drilling fluid for tests 1–11.

Mixing Sequence	Material/Additive	Mass (g)
1	H ₂ O	328
2	Na ₂ CO ₃	0.02
3	NaOH	0.25
4	Xanthan Gum	1.2
5	Poly-Anionic Cellulose, Low Viscosity	4.0
6	MgO	1.0
7	KCl	17.5
8	Bentonite	5.0
9	CaCO ₃ (D50 of 50 μm)	30.0
10	With or without FIBER A or FIBER B at given concentration	8.0

Table A2. Dry sieving of drilling fluid additives for tests 1–11.

Additive	<90 μm	90–180 μm	>180 μm
CaCO ₃	74.2%	24.8%	1.0%
FIBER A	56.3%	30.6%	13.1%
FIBER B	29.5%	56.5% *	13.9%

* When sieving of FIBER B it was noted that the particles had some magnetic properties. Visual inspection indicated that this might have increased amount of product collected in 90 μm sieve.

Table A3. Wet sieving of drilling fluid sample with additives before and after high-shear degradation for tests 1–11.

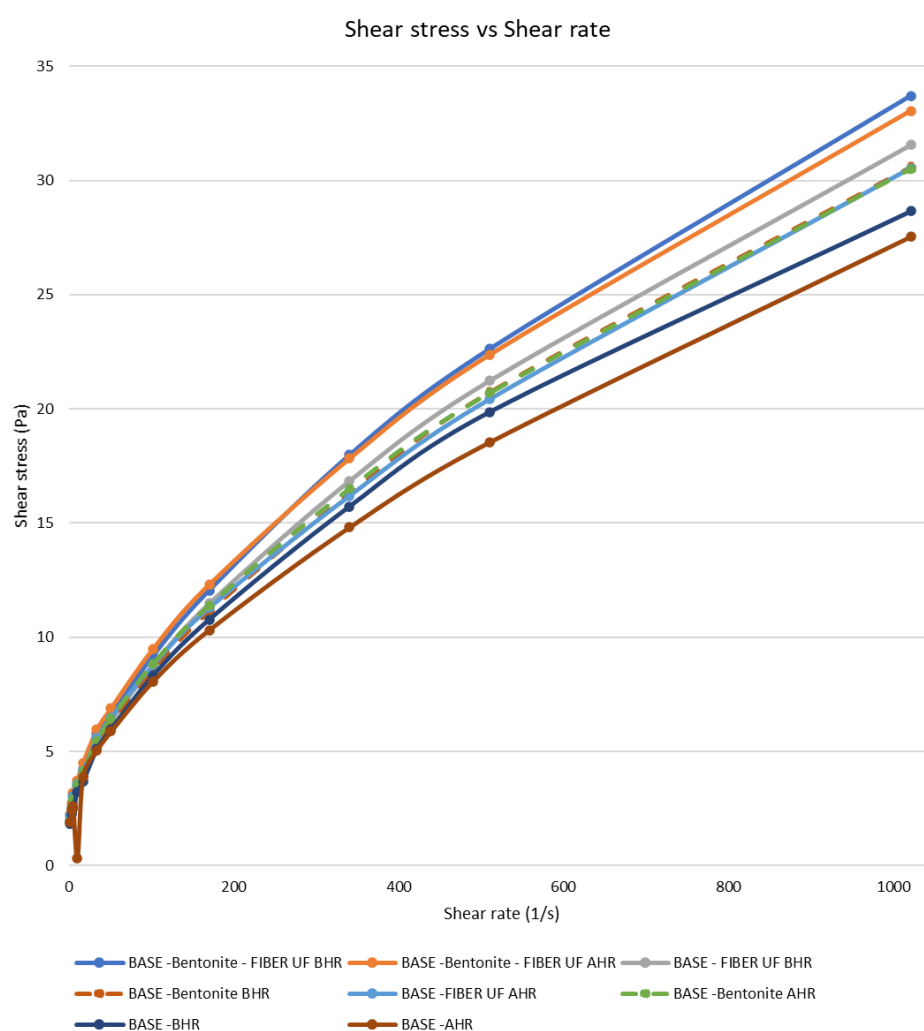
Wet Sieving before and after High-Shear Degradation	<90 μm	>90 μm
CaCO ₃ Sample #1, normal mixing	84.3%	15.7%
CaCO ₃ Sample #2, normal mixing	84.2%	15.8%
CaCO ₃ Sample #1, 30 min high-shear mixing	90.3%	9.7%
CaCO ₃ Sample #2, 30 min high-shear mixing	90.8%	9.2%
FIBER A Sample #3, normal mixing	53.4%	46.6%
FIBER A Sample #4, normal mixing	53.5%	46.5%
FIBER A Sample #5, 30 min high-shear mixing together with bentonite	38.6%	61.4%
FIBER A Sample #4, 30 min high-shear mixing	52.9%	47.1%

Table A4. Disc mass measurements in dry condition before and after whole test sequence for tests 1–11.

Test with Changes in Disc Mass	Original Disc Mass (g)	Final Disc Mass (g)	Mass Increase (g)
1, Base fluid (with bentonite and CaCO ₃), normal mixing, 120 μm disc	50.098	50.106	0.008
2, Base fluid, high-shear mixing, 120 μm disc	50.069	50.078	0.009
3, Base fluid, normal mixing, 250 μm disc (TOTAL LOSS)	50.249	50.329	0.080
4, Base fluid plus FIBER A, normal mixing, 120 μm disc	50.419	50.425	0.006
5, Base fluid plus FIBER A, high-shear mixing, 120 μm disc	49.970	49.988	0.018
6, Base fluid plus FIBER A, normal mixing, 250 μm disc	50.624	50.671	0.047
7, Base fluid plus FIBER A, high-shear mixing, 250 μm disc	50.457	50.647	0.190
8, Base fluid plus FIBER B, normal mixing, 120 μm disc	49.789	49.791	0.002
9, Base fluid plus FIBER B, high-shear mixing, 120 μm disc	49.927	49.929	0.002
10, Base fluid plus FIBER B, normal mixing, 250 μm disc	50.139	50.484	0.345
11, Base fluid plus FIBER B, high-shear mixing, 250 μm disc	50.204	50.423	0.219

Table A5. Recipe and mixing sequence of base fluid 2 for tests 12–15.

Mixing Sequence	Material/Additive	Mass (g)
1	H ₂ O	328
2	Na ₂ CO ₃	0.02
3	NaOH	0.25
4	Xanthan Gum	1.2
5	Poly-Anionic Cellulose, Low Viscosity	4.0
6	MgO	1.0
7	KCl	17.5
8	With or without Bentonite at given concentration	10.0
9	With or without FIBER UF at given concentration	5.0

**Figure A1.** Rheology before hot-rolling (BHR) and after hot-rolling (AHR) of fluids for tests 12–15.

Appendix B

Procedure for measuring change in disc mass and change in permeability and relevant calculations.

1. Mix drilling fluid according to the recipe;
2. Measure pH and rheology;

3. Hot-roll and if applicable degrade by high-shear stirring or other degradation method;
4. Measure pH and rheology after hot-rolling and any degradation;
5. Mark and weigh disc in dry condition using the moisture analyzer (M_b). Moisture analyzer shall be set to dry disc at 105 °C until change in mass is less than 1 mg/60 s;
6. Optional step: place disc in acrylic cell and measure air temperature and flowrate at different pressures to calculate average permeability to air (K_{ab});
7. Optional step: place disc in acrylic cell and place arrangement with water in vacuum (circa −0.96 bar for 5 min) to remove any air from disc or water. Flow thereafter water through disc and measure water temperature and flowrate at different pressures to calculate average permeability to water (K_{wb});
8. Soak disc in brine (40 g NaCl per 1000 g freshwater) in vacuum;
9. Conduct HTHP test at desired pressure, typically 3.45 MPa (500 psi) or 6.9 MPa (1000 psi), and measure both volume (V_f) and mass (M_f) of fluid filtrate at point in time of 15 s, 30 s, 1 min, 2 min, 3 min, 5 min, 10 min, 15 min, 20 min and 30 min (V_f). Calculate fluid filtrate density;
10. Weigh disc with filter-cake and observe filter-cake;
11. Place disc in acrylic cell and reverse flow with 1 L (40 g NaCl per 1000 g water) heated to 60 °C and then with 1 L water heated to 60 °C. Note pressure required to enable reverse flow through disc;
12. Optional step: place disc in breaker fluid for required time and at required temperature. Place disc in acrylic cell and flow disc with 1 L water at ambient temperature to remove any dissolved filter-cake residue;
13. Optional step: place disc in acrylic cell and place arrangement with water in vacuum to remove any air from disc or water. Flow thereafter water through disc and measure water temperature and flowrate at different pressures to calculate average permeability to water (K_{wa});
14. Weigh disc in dry condition using moisture analyzer (M_a) using the same settings as in step 5;
15. Optional step: place disc in acrylic cell and measure air temperature and flowrate at different pressures to calculate average permeability to air (K_{aa}).

Depending on the number of optional steps included in the procedure, it enables collection of a large amount of data in addition to observing the filter-cake and the fluid filtrate volume V_f .

The moisture analyzer used for weighing the discs was set to heating the discs to 105 °C and continue drying until the mass change due to moisture evaporation was less than 1 mg per 60 s. The drying process then stopped automatically, and the mass of the disc displayed. The precision of the instrument is 1 mg. The change in disc mass was then simply calculated as:

$$(M_a) - (M_b) = M_{\text{change}}$$

By placing a digital weight under the graduated cylinder used to measure fluid filtrate, it was possible to simultaneously record the mass of the fluid filtrate and read the volume of the filtrate. This enabled a precise estimation of the fluid loss profile and calculating the fluid filtrate density (D_f), calculated as:

$$(M_f)/(V_f) = (D_f)$$

The permeability was calculated as an average of multiple readings within certain flow-rate ranges. Darcy's law was used in a rearranged form as follows:

$$K = \eta \frac{Q * \Delta L}{A * \Delta P}$$

where K is the calculated permeability coefficient (m^2), η is the viscosity of the fluid ($Pa * s$), Q the fluid flowrate (m^3/s), ΔL the disc thickness (m), A the areal of flow into the disc and ΔP the pressure differential over the disc (Pa).

References

1. ANSI/API 13B-1. In *Recommended Practice for Field Testing Water-based Drilling Fluids*, 5th ed.; API Publishing Services: Washington, DC, USA, 2019.
2. Alsaba, M.; Nygaard, R.; Hareland, G. AADE-14-FTCE-25. In *Review of Lost Circulation Materials and Treatments with an Updated Classification*; AADE: Houston, TX, USA, 2014.
3. Jeennakorn, M.; Alsaba, M.; Nygaard, R.; Saasen, A.; Nes, O.-M. The effect of testing conditions on the performance of lost circulation materials: Understandable sealing mechanism. *J. Pet. Explor. Prod. Technol.* **2018**, *9*, 823–836. [[CrossRef](#)]
4. Jeennakorn, M.; Nygaard, R.; Nes, O.-M.; Saasen, A. Testing conditions make a difference when testing LCM. *J. Nat. Gas Sci. Eng.* **2017**, *46*, 375–386. [[CrossRef](#)]
5. Alshubbar, G.; Nygaard, R.; Jeennakorn, M. The effect of wellbore circulation on building an LCM bridge at the fracture aperture. *J. Pet. Sci. Eng.* **2018**, *165*, 550–556. [[CrossRef](#)]
6. Alsaba, M.; Nygaard, R.; Saasen, A.; Nes, O.M. *Lost Circulation Materials Capability of Sealing Wide Fractures*; SPE-170285-MS; SPE International: Houston, TX, USA, 2014.
7. Khalifeh, M.; Klungtvedt, K.R.; Vasshus, J.K.; Saasen, A. *Drilling Fluids—Lost Circulation Treatment*; SPE-195609-MS; SPE Norway: Bergen, Norway, 2019.
8. Saasen, A.; Hodne, H.; Ronæs, E.; Aarskog, S.A.; Hetland, B.; Løvereide, M.B.; Mohammadi, R. *Wood Fibre Based Lost Circulation Materials*; OMAE2018-77662; ASME: Madrid, Spain, 2018.
9. Lee, L.; Taleghani, A.D. Simulating Fracture Sealing by Granular LCM Particles in Geothermal Drilling. *Energies* **2020**, *13*, 4878. [[CrossRef](#)]
10. Enstad, G. On the theory of arching in mass flow hoppers. *Chem. Eng. Sci.* **1975**, *30*, 1273–1283. [[CrossRef](#)]
11. Whitfill, D. In Proceedings of the Lost Circulation Material Selection, Particle Size Distribution and Fracture Modelling with Fracture Simulation Software, SPE-115039-MS, IADC/SPE, Jakarta, India, 25–27 August 2008.
12. Alsaba, M.; Nygaard, R.; Saasen, A.; Nes, O.M. Experimental investigation of fracture width limitations of granular lost circulation materials, 2015. *J. Petrol. Explor. Prod. Technol.* **2016**, *6*, 593–603. [[CrossRef](#)]
13. Alsaba, M.; Aldushaishi, M.; Jeennakorn, M.; Nygaard, R.; Saasen, A.; Nes, O.M. *Sealing Pressure Prediction Model for Lost Circulation Treatments Based on Experimental Investigations*; AADE-17-NTCE-21; American Association of Drilling Engineers: Houston, TX, USA, 2017.
14. Hoxha, B.B.; Yang, L.; Hale, A.; van Oort, E. *Automated Particle Size Analysis using Advanced Analyzers*; AADE-16-FTCE-78; AADE: Houston, TX, USA, 2016.
15. Pitoni, E.; Ballard, D.A.; Kelly, R.M. *Changes in Solids Composition of Reservoir Drill in Fluids during Drilling and the Impact on Filter Cake Properties*; SPE 54753; SPE International: The Hague, The Netherlands, 1999.
16. Green, J.; Patey, I.; Wright, L.; Carazza, L.; Saasen, A. *The Nature of Drilling Fluid Invasion, Clean-Up, and Retention during Reservoir Formation Drilling and Completion*; SPE-185889-MS; SPE Bergen: Bergen, Norway, 2017.
17. Czuprat, O.; Dahle, B.O.; Dehmel, U.; Ritschel, R.; Storhaug, J.; Adrian, T.; Patley, I. *Systematic Selection of Drill-in and Completion Fluids for Development of the Dvalin HT Gas Field*; SPE-195601-MS; SPE Norway: Bergen, Norway, 2019.
18. Khan, R.; Kuru, E.; Tremblay, B.; Saasen, A. Extensional Viscosity of Polymer Based Fluids as a Possible Cause of Internal Cake Formation. *Energy Sources A* **2007**, *29*, 1521–1528. [[CrossRef](#)]
19. Cobianco, S.; Bartosek, M.; Lezzi, A.; Previde, E. *New Solids-Free Drill.in Fluid for Low Permeability Reservoirs*; SPE-64979; SPE: Houston, TX, USA, 2001.
20. Nelson, P.H. Pore-throat sizes in sandstones, tight sandstones, and shales. *AAPG Bull.* **2009**, *93*, 329–340. [[CrossRef](#)]
21. Civan, F. *Reservoir Formation Damage 2020*; Gulf Professional Publishing: Waltham, MA, USA, 2020; pp. 1–6, ISBN 978-0-12-801898-9.
22. ANSI/API 13B-2. In *Recommended Practice for Field Testing Oil-Based Drilling Fluids*, 5th ed.; API Publishing Services: Washington, DC, USA, 2014.